

# All for One, and One for All: UrbanSyn Dataset, the third Musketeer of Synthetic Driving Scenes

Jose L. Gómez<sup>1\*</sup>, Manuel Silva<sup>1,5\*</sup>, Antonio Seoane<sup>5</sup>, Agnès Borrás<sup>1</sup>,  
Mario Noriega<sup>1</sup>, German Ros<sup>3</sup>, Jose A. Iglesias-Guitian<sup>2,5</sup>, Antonio M. López<sup>1,4</sup>

<sup>1</sup> Computer Vision Center (CVC), <sup>2</sup> CITIC - Centre for ICT Research, <sup>3</sup> NVIDIA,

<sup>4</sup> Computer Science Department, Universitat Autònoma de Barcelona (UAB),

<sup>5</sup> Universidade da Coruña (UDC)

Contact emails: jlgomez@cvc.uab.cat, m.silval@udc.es, antonio.seoane@udc.es,  
agnes.borras@cvc.uab.cat, mnoriega@cvc.uab.cat, grossanchez@nvidia.com,  
j.iglesias.guitian@udc.es, antonio@cvc.uab.es



Fig. 1: Samples from the Musketeers dataset: GTAV [1], Synscapes [2], and UrbanSyn (ours).

**Abstract**—We introduce UrbanSyn, a photorealistic dataset acquired through semi-procedurally generated synthetic urban driving scenarios. Developed using high-quality geometry and materials, UrbanSyn provides pixel-level ground truth, including depth, semantic segmentation, and instance segmentation with object bounding boxes and occlusion degree. It complements GTAV and Synscapes datasets to form what we coin as the ‘Three Musketeers’. We demonstrate the value of the Three Musketeers in unsupervised domain adaptation for image semantic segmentation. Results on real-world datasets, Cityscapes, Mapillary Vistas, and BDD100K, establish new benchmarks, largely attributed to UrbanSyn. We make UrbanSyn openly and freely accessible.

## I. INTRODUCTION

Human data labeling is a major bottleneck for training and validating many deep perception models. To solve vision tasks, datasets of synthetic images have attracted a great deal of interest [3], [4], [1], [2]. They come with many

**Funding Acknowledgements:** This work has been supported by the Spanish grants Ref. PID2020-115734RB-C21 (ADA/SSL-ADA subproject) and PID2020-115734RB-C22 (ADA/PGAS-ADA subproject) both funded by MCIN/AEI/10.13039/501100011033. Antonio M. López acknowledges the financial support to his general research activities given by ICREA under the ICREA Academia Program. CVC’s authors acknowledge the support of the Generalitat de Catalunya CERCA Program and its ACCIO agency to CVC’s general activities. Jose A. Iglesias-Guitian acknowledges the financial support to his general research activities given by UDC-Inditex InTalent programme, the Spanish Ministry of Science and Innovation (AEI/RYC2018-025385-I), and Xunta de Galicia (ED431F 2021/11, EU-FEDER ED431G 2019/01).

\* Jose L. Gómez and Manuel Silva are co-first authors.

types of automatically generated ground truths (i.e., labels), and, in contrast to human-produced labels, synthetic ones are accurate and consistent across images. However, since deep models trained on synthetic images must later perform in real-world images, the synth-to-real domain gap must be addressed, which remains an open research topic [5], [6], [7]. In fact, domain gaps also exist among real-world images captured by different camera sensors. However, synth-to-real domain adaptation is especially relevant because it opens the door to minimizing costly and not fully safe autonomous driving developments in the real world. For instance, in an autonomous driving simulator, we can force desired traffic scenarios that are difficult to observe in the real world by random roaming and train perception models with data captured during such simulations. Research on synth-to-real domain adaptation pursues to develop methods to adapt these models to perform in the real world, preferably in an unsupervised manner. As argued in other AI sub-fields [8], [9], we must rely on reasonably strong baselines to avoid illusory gains when developing new proposals for a given task. In our case, this means starting with reasonably accurate synthetic-only baseline models to bridge the synth-to-real domain gap. The prevailing approach to addressing the synth-to-real gap typically involves focusing on a single synthetic dataset at a time, which leads to less-than-optimal results. It is important to note that when dealing exclusively with real-world labeled images, training complex models on datasets compiled from

various sources has been shown to enhance their accuracy compared to training them on each source separately. This increase in accuracy is not produced by the larger number of training samples but by the additional diversity derived from the use of different data sources. This has been observed for core visual tasks such as semantic segmentation [10], object detection [11], and depth estimation [12].

Driven by the idea of multi-source approaches [13], [14], [15], [16], we introduce the UrbanSyn dataset. A collection of highly realistic synthetic images of urban scenarios generated semi-procedurally. UrbanSyn targets computer vision tasks in driving domains and features labels, including pixel-wise instance and semantic masks, depth, and bounding boxes for objects with occlusion degree. This novel dataset aims at complementing other publicly available synthetic datasets such as GTAV [1] and Synscapes [2], addressing the synth-to-real domain gap from a multi-source perspective. To achieve such a complementarity, UrbanSyn is based on unbiased path tracing instead of the video game deferred rendering technique utilized in GTAV. This results in rendering real-world imperfections in a more realistic manner. Moreover, while Synscapes is also more realistic than GTAV, UrbanSyn generation goes beyond by simulating atmospheric effects through physics-based light-transport simulation in participating media. Additionally, UrbanSyn is generated from totally new 3D environments and assets. All this means that UrbanSyn images show scenes different from those in GTAV and Synscapes in terms of content and appearance.

In this paper, we demonstrate the value of UrbanSyn by addressing semantic segmentation, a challenging task [17], [18], [19] that has proven to be key for the correct performance of many autonomous driving solutions [20], [21], [22]. Note that onboard semantic segmentation involves assigning a traffic-relevant semantic class (e.g., Vehicle, Pedestrian, Road, etc.) to each pixel of an image captured for the automatic understanding of the vehicle’s surroundings and so for performing safe driving maneuvers. Deep learning models are the most effective way to accomplish this visual task. Thus, it is essential to gather training images that bring diversity and accurately labeled semantic information. However, obtaining this labeled data is a time-consuming process, taking 60-90 minutes per image due to the manual human labeling involved. UrbanSyn brings accurate pixel-wise semantic labels for onboard images depicting diverse urban environments and objects. When used individually, we show that UrbanSyn gives rise to stronger semantic segmentation baselines than GTAV and Synscapes datasets. But most importantly, the strongest baselines arise when GTAV, Synscapes, and UrbanSyn are combined. Inspired by Alexandre Dumas, we refer to the combination of these datasets as *The Three Musketeers*<sup>1</sup> (Figure 1). Our experiments make use of modern and relevant approaches, including DeepLab V3+ [23] and SegFormer [24], evaluated in challenging real-world datasets, such as Cityscapes [25], BDD100K [26], and Mapillary Vistas [27]. We also show that our claim remains valid when these approaches are used for synth-to-real semantic self-labeling. To show this, we rely on

several synth-to-real unsupervised domain adaptation (UDA) methods. In particular, we use the HRDA [28] and co-training [16] frameworks. We show that adding UrbanSyn boosts semantic segmentation results to the state-of-the-art on synth-to-real UDA for semantic segmentation. On the other hand, we encourage researchers to not only use UrbanSyn for such a task but also for others requiring labels, for instance, segmentation, object detection, and depth estimation. Accordingly, we make UrbanSyn publicly available to the research community for free. In this regard, it is also important to note that, to generate images that can be used for training AI models, the digital assets used to create UrbanSyn have been carefully curated to ensure they are legally usable for that purpose.

The rest of the paper is organized as follows: Section II overviews the most related works, placing ours in context. Section III details the main components involved in the generation of UrbanSyn. Section IV shows the usefulness of UrbanSyn for synth-to-real UDA in semantic segmentation. Finally, Section V summarizes the work presented in this paper and outlines related future work.

## II. RELATED WORK

### A. Synthetic datasets of driving scenarios.

The use of synthetic datasets for visual machine learning is becoming increasingly popular for many tasks in computer vision, mostly motivated by its potential to reduce the need for expensive and time-consuming manual image labeling. A recent survey [29] provides a comprehensive overview of various image synthesis approaches according to their modeling and rendering procedures as well as their applications in computer vision. While a whole range of synthetic datasets exists for different domains providing various types of labeled information [30], [31], [32], [33], we focus here on those presenting driving scenarios.

Using driving simulators as platforms to produce large amounts of automatically labeled images has been successfully proposed in the last decade [34], [4], [1], [35], [3], [36], [30]. However, while these approaches can rapidly generate thousands of labeled images, their results often lack a photorealistic level. This can be attributed to two factors: i) the overall quality used to model the underlying 3D assets, which often trades level of detail in exchange for simulation speed; and ii) the use of real-time game engines for rendering, which often employ trade-off implementations to approximate complex global illumination, reflections, shadows, and camera lens effects with less accuracy. Popular datasets generated under these trade-offs are GTAV [1], SYNTHIA [4], Virtual KITTI [3], and those based on CARLA simulator [36].

A recent trend to increase the realism of the generated images is to employ high-quality 3D assets together with offline Monte Carlo ray-tracing algorithms like path tracing [37], [2]. This was the case of Synscapes [2], in which the gained photorealism came with an extra rendering cost. Another relevant aspect is the authoring cost employed in pursuing realistic layouts. Several works opted to incorporate procedural modeling in their pipelines; e.g., Synscapes incorporated a procedural scene generator, as well as ProcSy [38], which

<sup>1</sup>All synthetic datasets for one, and one for all.

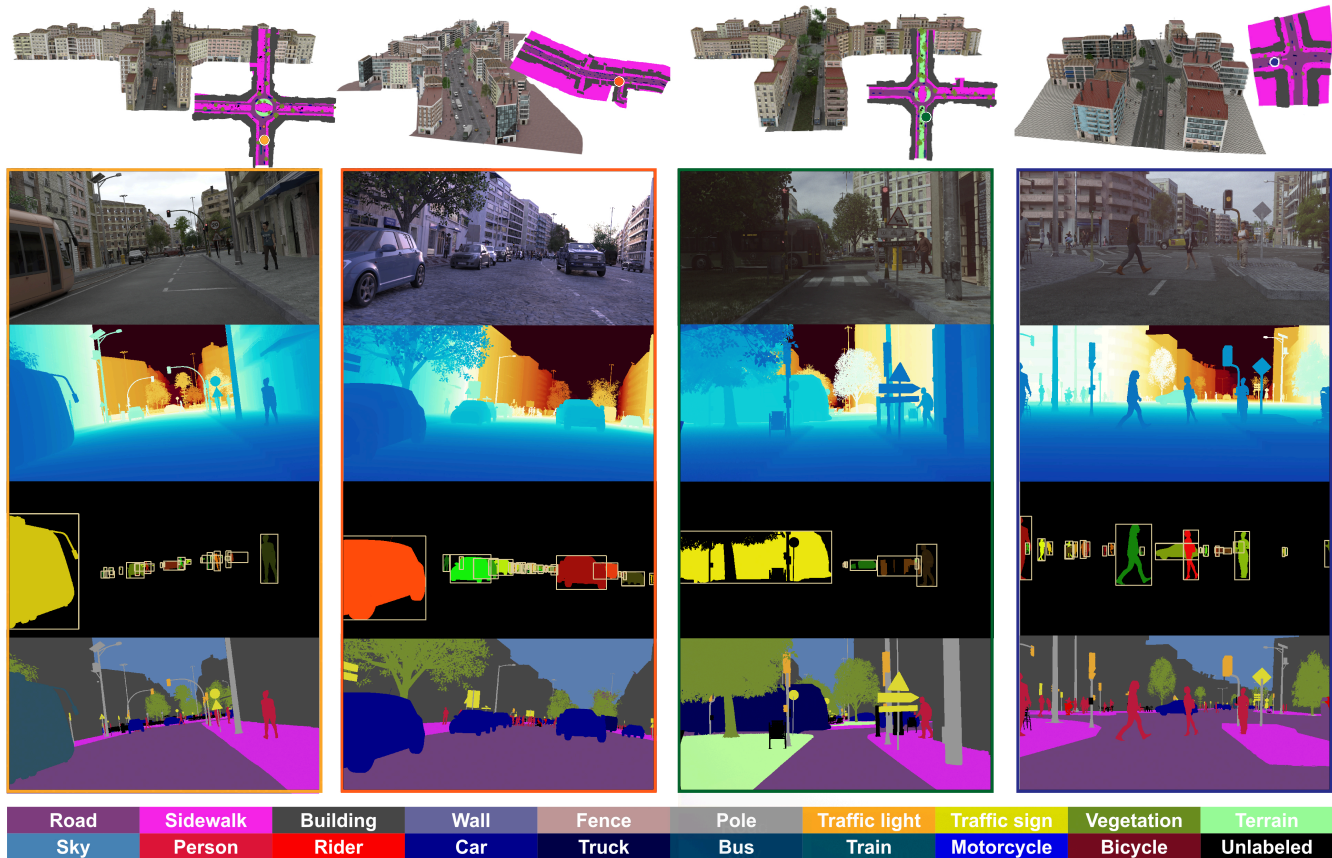


Fig. 2: UrbanSyn covers 4 different ODDs. It supports different lighting conditions, enabling atmospheric participating media (e.g., columns 3 and 4), procedurally generating different building landscapes, and shuffling locations and materials of assets. From top to bottom, we see a top view of the ODDs, RGB images captured around the indicated circles within the ODDs, corresponding depth maps (pseudo-color), object instances with their bounding boxes, and per-pixel class semantic labels.

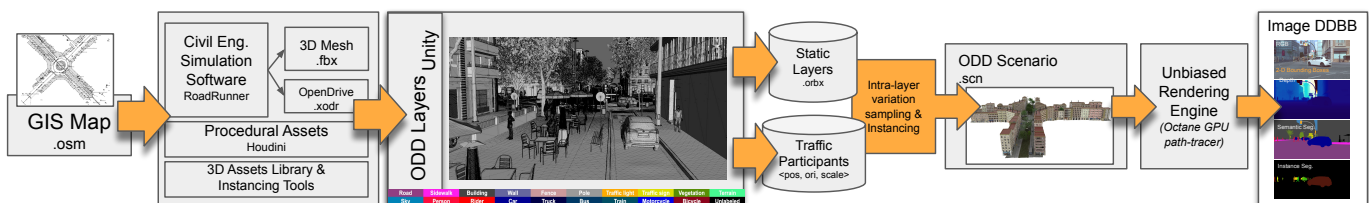


Fig. 3: UrbanSyn content generation pipeline overview. Our builder scripts combine real GIS data with procedurally generated content and a 3D library of custom and commercial assets to create layers containing configurable content variations.

delegated that task to CityEngine [39]. Another alternative consists of automatically synthesizing scene layouts tailored to solve downstream tasks, e.g., semantic segmentation. MetaSim [40] aimed at automatically tuning parameters given a target collection of real images in an unsupervised way, while MetaSim 2 [41] aims at learning the scene structure in addition to parameters. In both cases, automatically labeled images were generated through a graphics engine sharing trade-offs similar to those presented for most driving simulators.

### B. Synth-to-real semantic segmentation.

Using synthetic images to train semantic segmentation models implies addressing the synth-to-real domain gap, which has

attracted a significant amount of research in recent years. We advise readers to consult [18] for a comprehensive review. In this context, it is assumed that no human-provided labels are available for real-world images; thus, synth-to-real semantic segmentation becomes a problem of unsupervised domain adaptation (UDA).

In this context, UDA methods are based on two general ideas, taken in isolation or combination. One idea is to perform a synthetic-real domain alignment of the input/features/output of the deep model under training. The other idea is to perform self-labeling (i.e., producing pseudo-labels) of the real-world images for their use in re-training/back-propagation loops. Attending to how coupled to the underlying deep model

architecture is the implementation of these ideas, we find model-centric [42], [43], [44], [45], [46], [14], [47], [48], [49], [50], [51], [52], [53], [28], [54] and data-centric [55], [56], [57], [58], [59], [15], [16] methods. Model-centric methods have been developed on top of a particular deep architecture (by accessing specific internal layers or modifying its loss function). Data-centric methods treat deep models pretty much as black boxes and mainly focus on assessing and guaranteeing the reliability of the predicted pseudo-labels. Model- and data-centric methods can be complemented with tailored data augmentation techniques [60], [61], [62], with image-to-image translation [63], [64], [65], and with LAB color space alignment which, in line with findings regarding color spaces and robustness of deep models [66], can meaningfully reduce the synth-to-real domain gap [15], [16].

Most works use Cityscapes as real-world (target) domain, while SYNTHIA, GTAV, and/or Synscapes are used as synthetic (source) domains. The predominant experimental setting corresponds to using a single synthetic dataset as the source domain. However, some works have shown the convenience of relying on multiple synthetic sources [13], [14], [15], [16] to reduce the synth-to-real domain gap, which is in agreement with findings in the pure real-world setting [10].

### C. In this paper.

We introduce UrbanSyn, a novel dataset for autonomous driving research generated by combining high-quality 3D assets, semi-procedural tools for scene layout generation, and path tracing rendering techniques to produce labeled images with a high degree of photorealism. By design, UrbanSyn is compact and brings differences from GTAV and Synscapes regarding road layouts, background content, and traffic participants. To show its usefulness, besides providing synthetic-only semantic segmentation baseline results, we use UrbanSyn for running synth-to-real UDA methods. We use the state-of-the-art HRDA [28] to represent model-centric methods and the state-of-the-art co-training [16] to represent data-centric methods. As the real-world target domain, our experiments not only consider Cityscapes as in most previous literature but also the more challenging BDD100K and Mapillary Vistas datasets. The obtained results confirm that both in isolation and as part of the Three Musketeers dataset, UrbanSyn fosters synth-to-real semantic segmentation.

## III. URBANSYN, THE NEW MUSKETEER

This section summarizes different aspects concerning the generation of UrbanSyn, including the construction of our Operational Design Domains (ODDs) and some image rendering details. Overall, as novel real-world datasets are different from previous ones because they were acquired in different real-world areas using different camera sensors and lighting conditions, such differences also apply to UrbanSyn compared to GTAV and Synscapes, making them inherently complementary.



Fig. 4: Rendering results using unbiased path tracing (PT) with different sample counts. We set the adaptive sampling to use a maximum of 256 spp. Adaptive sampling and denoising help reduce undesired PT noise and large rendering times.

### A. Dataset features

The UrbanSyn dataset provides photorealistic color images, paired with their ground-truth depth maps, pixel-level semantics and instance segmentation, as well as 2D object bounding boxes indicating their occlusion degree as a percentage value w.r.t. the whole object within the camera frustum. We adhere to the common 19 classes of Cityscapes as the established de facto standard. Please check Figure 2 to see some image examples and their corresponding labeled information.

UrbanSyn aims to model real-world imperfections affecting both the geometry and the material appearance of its assets. In contrast to GTAV, we utilize unbiased path tracing instead of videogame deferred rendering. When compared to Synscapes, we enrich realism by simulating atmospheric effects like urban air pollution through physics-based light-transport simulation in participating media. In addition, we exploit procedural assets with randomized geometries and materials to enhance the variability of certain assets (e.g., buildings), and we also simulate different types of vehicle lights, all intending to elevate UrbanSyn to a new level of photorealism.

Moreover, UrbanSyn has been meticulously generated to optimize diversity and training value, balancing efficiency and quality and resulting in a more compact dataset than its predecessors. In particular, we showcase distinctive scene configurations, assets, and illumination profiles while minimizing redundant images as much as possible (e.g., we avoid capturing similar views under similar environment conditions). As a consequence, UrbanSyn consists of 7,539 images, making it easy to share and store and being aligned with the *train on less data* tip for decarbonizing AI development [67]. As we will see in Section IV, despite its compactness, UrbanSyn gives rise to the most accurate models for image semantic segmentation.

### B. Data generation pipeline

The designed pipeline to generate UrbanSyn, summarized in Figure 3, allowed us to seamlessly integrate highly realistic and curated scene layouts with procedurally-generated content based on high-quality assets and materials. Similarly to Synscapes or ProcSy, our dataset is mostly procedurally generated. However, our approach uses real maps from GIS sources, i.e., OpenStreetMaps (OSM), to model realistic scenario layouts.

The main roads, lanes, and sidewalks are traced over using Mathworks RoadRunner, as well as potential locations of traffic signs or traffic lights. Then, a parameterized in-house builder script parses and instantiates a 3D variation of a given scenario layout inside the Unity game engine. We mainly utilize Unity as our simulation engine to verify plausible spatial occupancy among all assets, e.g., to avoid geometry collisions. The system allows controlling per-class picking distributions in a statistically meaningful manner and supports per-asset weighted probabilities. Our approach assembles these scenarios by parts (layers), sampling from a predefined set of available 3D assets<sup>2</sup>, and automatically instancing procedural variations developed via Unity scripting and SideFX Houdini.

### C. Rendering details

The images presented in UrbanSyn were generated using OctaneRender’s implementation of unbiased path tracing [68], a widely used technique in computer graphics and the film industry [69]. However, one of the well-known side effects of Monte Carlo (MC) path tracing is its variance noise [70].

To generate UrbanSyn, we decided to employ adaptive sampling, a technique that adaptively dedicates more samples in those regions where the estimated MC variance noise is higher. We established a threshold of 128 samples-per-pixel (spp) to estimate the initial per-pixel variance and let the adaptive sampling algorithm decide where to continue calculating more samples for each pixel. To further reduce noise, we relied on OctaneRender’s built-in deep learning-based denoising [71]. This allowed us to significantly reduce the total rendering time per frame, from potentially several hours to just a hundred seconds, all at the expense of trading MC variance noise with some minimal bias introduced by the denoising. The overhead of the denoiser is almost negligible, as it requires only from 1 to 5 seconds per image. Thus, the images of UrbanSyn were rendered and denoised using a maximum of 256 spp. Figure 4 illustrates how renders using 256 spp and denoising could be perceptually very similar to unbiased PT renders with  $\times 4$  to  $\times 8$  more spp (e.g.1K or 2K spp).

While the specific parameters of the path-tracing algorithm could be adjusted according to the target scenario, we utilized a set of predefined and recommended parameter values that worked well across the wide variety of scenarios covered by UrbanSyn. For example, the maximum amount of diffuse and specular (glossy) bounces was set to a maximum of 4 bounces. The cost of rendering one frame also depends on the ODD.

### D. Operational Design Domains (ODDs)

Using the aforementioned pipeline, we can generate different variations and asset distributions within our ODDs. For UrbanSyn, we have considered four, inspired by common real traffic layouts (see the top row of Figure 2). Table I details the number of images, average, and total rendering time for each ODD. We can observe that using a participating medium

TABLE I: UrbanSyn detailed characteristics per ODD. Rendered using two NVIDIA RTX 3090 GPUs in parallel.

#ODD	Num. of images	Use Part. Media	Average rendering per image	Total time
ODD 1	1,319	No	36.96s	13h 32m
ODD 2	1,369	Yes	120.82s	45h 56m
ODD 3	2,905	No	24.55s	19h 48m
ODD 4	1,946	Yes	87.95s	47h 32m
Total	7,539	Y:43%, N:57%	69.17s	132h 46m

has a huge impact on render times. Additionally, Table II details the intrinsic variability of the ODDs, detailing the number of assets, materials, and variations for each class. We build the scenes used for rendering UrbanSyn, combining these assets to obtain the greatest amount of diversity while preserving the plausibility of the result. To maintain sufficient control over random shuffling, we precomputed a series of intra-layer variations for static elements and conducted random sampling over them. After that, dynamic traffic participants are positioned and later instantiated directly within the rendering engine. This alternative produced enough variations for our purpose of generating single images.

The unbiased path tracer then takes the generated scenarios as input and produces the labeled images. Multiple steps are involved before generating the final RGB images, including tone-mapping and gamma transformations, to convert them to low-dynamic range (LDR) in the desired RGB color space.

### E. UrbanSyn brings diversity

GTAV was acquired from a video game, bringing all the well-known limitations related to real-time simulation (e.g., limited degrees of graphics realism, and a limited number of object instances present at once in the scene). Additionally, GTAV suffers a clear bias towards American-style street maps and cars. Synscapes *was designed to closely resemble the Cityscapes dataset in structure and content* as stated by their authors [2]. Unlike GTAV, the scenarios generated in Synscapes are biased toward German cities. It is based on small maps, making use of a limited variety of materials, simplified procedural roads and buildings, missing real-world imperfections, and thus striking CGI uncanny perfection. Moreover, images tend to be overpopulated for all classes lacking in realism on scene composition. On the other hand, Synscapes offered higher image quality by utilizing unbiased path-tracing rendering.

UrbanSyn has been conceived for diversity since its conception, not being tailored for any specific real-world dataset. Having in mind that more synthetic data does not necessarily guarantee a better model performance [72], we defined a set of clear requirements for the newly proposed dataset: i) it should achieve high graphics realism, at the level of Synscapes or beyond, to help to reduce synth-to-real visual domain shift; ii) the images should depict scenarios unseen in previous datasets, including real-world imperfections; iii) we aimed for semi-procedurally generated content seamlessly integrated with high-quality assets, so to get the better of both worlds in terms of realism and the covered variety. The achievement of these requirements has made UrbanSyn a great complement for

<sup>2</sup>These assets were developed in-house or acquired with licenses that allow UrbanSyn redistribution under the CC-BY-SA 4.0 license.

TABLE II: Details of the intrinsic variability we have implemented to capture the images composing UrbanSyn. Camera poses correspond to those commonly used onboard a regular car, either looking forward or backwards, with orientation variations.

ODD	Layers	Classes	Intra-class Variations	Observations	# Source Assets	# Materials	# Cameras
<b>Roundabout ODD 1 and ODD 2 32 scenarios</b>	E	Sky (Environment Lighting)	100	Each HDR asset is rotated 4 times	25	1 per Sky	[18-26] per scene
	S01	Road	13	RoadRunner + Procedural Displacement Tool	1 Road	7 (+decals +rails)	
	S02	Sidewalk	10 (+10)	RoadRunner + Procedural Displacement Tool	1 Sidewalk	10	
	S03	Vegetation, Terrain, Fence & Wall	4 (+4)	Commercial + Custom 3D Models	11 Trees, 2 Terrains, 7 Fences, 4 Walls	At least 1 per tree/terrain/fence/wall	
	S04	Building	13	Unity + Houdini Asset	8 Building Blocks & 31 Basements	24 base materials for building blocks and 18 base materials for basement	
	S05	Traffic-Sign & Pole	8	Procedural Tool for Traffic Signs	15 Plaques, 7 Pole	155 different signs * 3 noise levels = 466 materials	
	S06	Traffic-Light, Pole & Miscellaneous	4	Unity Scatter Tool	10 source Traffic light each one with multiple settings	3 to 6 colours per Traffic light	
	S07	Pole (Others)	4	Unity Scatter Tool	3 Bollards, 7 Street Lamps	1 per pole	
	S08	Miscellaneous	4 (+4)	Unity Scatter Tool	12 Miscellaneous Props	1 per prop	
	D01	Car (Van), Rider, Bike, Motorbike, Truck, Bus y Train	50	Commercial + Custom 3D Models + Procedural Scatter Tool (based on OpenDrive data)	5 Cars, 5 Trucks, 1 Bus, 1 Train 5 Bicycles, 4 Motorbikes, 12 Riders (6M+6W)	Random colors for Vehicles except Bikes and trains. 4 materials per model for trains. 3 material per model for bikes.	
D02	Pedestrian	4	Commercial 3D Models + Unity Scatter Tool	24 Man & 24 Woman	1 per pedestrian		
<b>L-intersections ODD 3 31 scenarios</b>	E	Sky (Environment Lighting)	100	Each HDR asset is rotated 4 times	25	1 per Sky	[80-150] per scene
	S01	Road	7	RoadRunner + Procedural Displacement Tool	1 Road	7 (+decals)	
	S02	Sidewalk	8	RoadRunner + Procedural Displacement Tool	1 Sidewalk	10	
	S03	Vegetation, Terrain, Fence & Wall	4	Commercial + Custom 3D Models	11 Trees, 2 Terrains, 7 Fences, 4 Walls	At least 1 per tree/terrain/fence/wall	
	S04	Building	6	Unity + Houdini Asset	8 Building Blocks(different than Poblenuou) & 31 Basements	24 base materials for building blocks and 18 base materials for basement	
	S05	Traffic-Sign & Pole	4	Procedural Tool for Traffic Signs	15 Plaques, 7 Pole	155 different signs * 3 noise levels = 466 materials	
	S06	Traffic-Light, Pole & Miscellaneous	4	Unity Scatter Tool	10 source Traffic light each one with multiple settings	3 to 6 colours per Traffic light	
	S07	Pole (Others)	4	Unity Scatter Tool	3 Bollards, 7 Street Lamps	1 per pole	
	S08	Miscellaneous	4	Unity Scatter Tool	12 Miscellaneous Props	1 per prop	
	D01	Car (Van), Rider, Bike, Motorbike, Truck, Bus y Train	21	Commercial + Custom 3D Models + Procedural Scatter Tool (based on OpenDrive data)	12 Cars, 7 Trucks, 3 Bus, 3 Train 5 Bicycles, 10 Motorbikes, 24 Riders (13M+11W)	Random colors for Vehicles except Bikes and trains. 4 materials per model for trains. 3 material per model for bikes.	
D02	Pedestrian	8	Commercial 3D Models + Unity Scatter Tool	40 Man & 40 Woman	1 per pedestrian		
<b>4-Way Intersection ODD 4 45 scenarios</b>	E	Sky (Environment Lighting)	100	Each HDR asset is rotated 4 times	25	1 per Sky	[38-64] per scene
	S01	Road	7	RoadRunner + Procedural Displacement Tool	1 Road	7 (+decals)	
	S02	Sidewalk	4	RoadRunner + Procedural Displacement Tool	1 Sidewalk	10	
	S03	Vegetation, Terrain, Fence & Wall	4	Commercial + Custom 3D Models	11 Trees, 2 Terrains, 7 Fences, 4 Walls	At least 1 per tree/terrain/fence/wall	
	S04	Building	6	Unity + Houdini Asset	8 Building Blocks(different than Poblenuou) & 31 Basements	24 base materials for building blocks and 18 base materials for basement	
	S05	Traffic-Sign & Pole	4	Procedural Tool for Traffic Signs	15 Plaques, 7 Pole	155 different signs * 3 noise levels = 466 materials	
	S06	Traffic-Light, Pole & Miscellaneous	4	Unity Scatter Tool	10 source Traffic light each one with multiple settings	3 to 6 colours per Traffic light	
	S07	Pole (Others)	4	Unity Scatter Tool	3 Bollards, 7 Street Lamps	1 per pole	
	S08	Miscellaneous	4	Unity Scatter Tool	12 Miscellaneous Props	1 per prop	
	D01	Car (Van), Rider, Bike, Motorbike, Truck, Bus y Train	25	Commercial + Custom 3D Models + Procedural Scatter Tool (based on OpenDrive data)	14 Cars, 7 Trucks, 3 Bus, 3 Train 5 Bicycles, 10 Motorbikes, 24 Riders (13M+11W)	Random colors for Vehicles except Bikes and trains. 4 materials per model for trains. 3 material per model for bikes.	
D02	Pedestrian	4	Commercial 3D Models + Unity Scatter Tool	40 Man & 40 Woman	1 per pedestrian		

GTAV and Synscapes. Thus, it makes sense to use UrbanSyn alone or as part of the Three Musketeers. Figure 5 details per-class statistics of pixel occupancy and percentage of images of the Three Musketeers. UrbanSyn is well-balanced and a trade-off between GTAV and Synscapes. On the one hand, it provides a more balanced variability and quantity than GTAV in classes such as Rider, Bus, Train, Motorcycle, and Bicycle. On the other hand, UrbanSyn maintains the scene realism and coherence, avoiding Synscapes practices to overpopulate all images always with every class on them (e.g., Synscapes have around 70% of images that contain class Train, unrealistic in a real-world urban scenario.)

#### IV. EXPERIMENTAL RESULTS

In this paper, we highlight the usefulness of UrbanSyn by focusing on one of its ground truths, namely the pixel-level class labels. These labels are crucial for conducting synth-to-real UDA to develop semantic segmentation models without human labeling. We conduct comprehensive experiments in this section to demonstrate the importance of these labels. In the rest of this section, we begin by explaining the standard experimental methodology applied to evaluate synth-to-real UDA settings, for either assessing new UDA protocols or new synthetic datasets as is our purpose in this paper. Next, we detail the datasets and evaluation metrics used in our experiments. After, we provide additional implementation details. Finally, we present the experiments and discuss the results

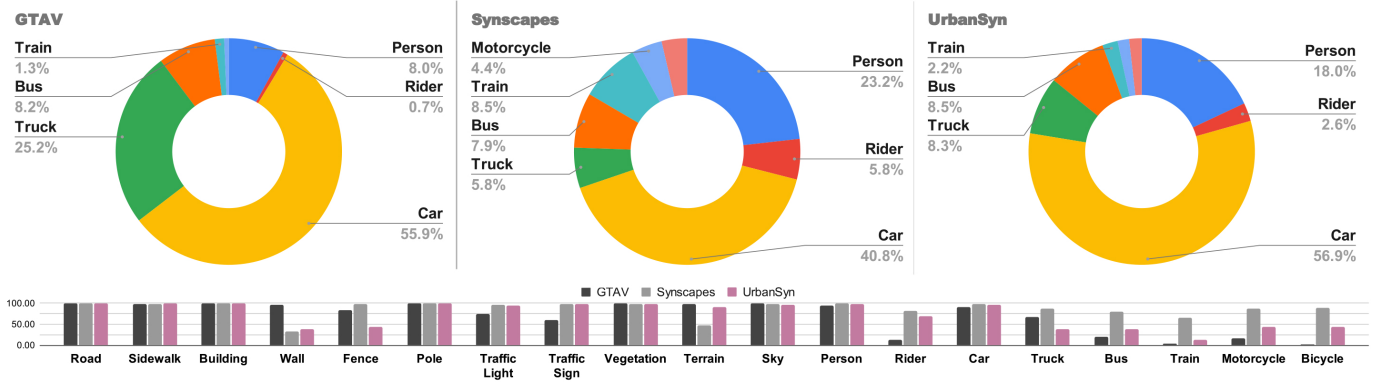


Fig. 5: Content statistics for the Musketeers dataset: (Top) Per-class pixel-occupancy distributions. Apparently, the three datasets show relatively similar distributions, sharing more than what could set them apart. (Bottom) Percentage of images containing samples of the given class. UrbanSyn is on par with Synscapes for certain classes, where both provide more examples than GTAV (e.g., Bus and Rider).

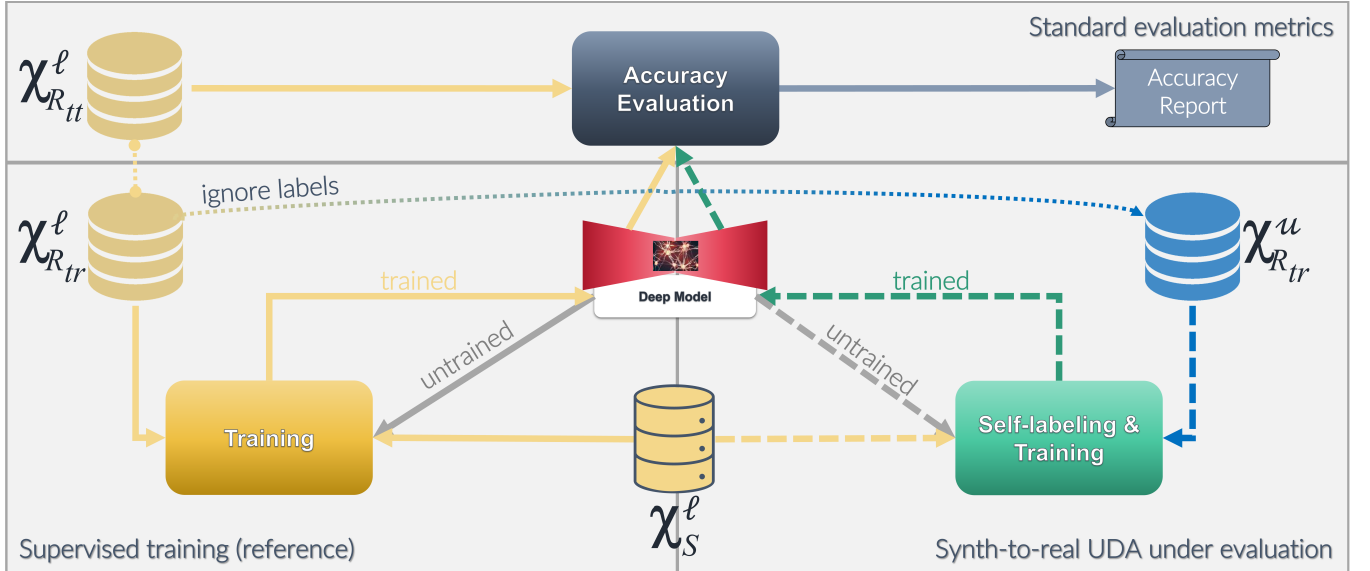


Fig. 6: Experimental evaluation methodology for synth-to-real UDA procedures. Please, refer to the main text in section IV-A for details.

obtained.

#### A. Experimental methodology

Figure 6 illustrates the standard experimental evaluation methodology used to assess synth-to-real UDA procedures, which we also adhere to in this paper. It is assumed that we have a deep model to be adapted, a source domain in the form of automatically labeled synthetic data,  $\mathcal{X}_S^l$ , and a target domain in the form of real-world unlabeled training data,  $\mathcal{X}_{R_{tr}}^u$ . In practice, to perform experiments, the real-world domain is composed of a training and a testing set,  $\mathcal{X}_{R_{tr}}^l$  and  $\mathcal{X}_{R_{te}}^l$  respectively. These are used by the research community for different types of tasks. For instance, in the case of synth-to-real UDA, the set  $\mathcal{X}_{R_{tr}}^l$  plays the role of  $\mathcal{X}_{R_{tr}}^u$  by ignoring its (human-provided) labels. Then, a standard training of the deep model using  $\mathcal{X}_{R_{tr}}^l$  is used as upper-bound reference for the synth-to-real UDA under evaluation; while an analogous

training based on  $\mathcal{X}_S^l$  is used as lower-bound reference. The goal of a synth-to-real UDA method is to use  $\mathcal{X}_S^l$  and  $\mathcal{X}_{R_{tr}}^u$  to obtain a similar (or better) performing deep model than if  $\mathcal{X}_{R_{tr}}^l$  is used as the training set. This process involves self-labeling  $\mathcal{X}_{R_{tr}}^u$ . To assess model accuracy irrespective of its training,  $\mathcal{X}_{R_{te}}^l$  and a standard evaluation procedure are used. The assumption is that good synth-to-real UDA procedures will be able to address the training of deep models for new unlabeled real-world datasets at least using the same synthetic data or improved versions of it.

This general methodology translates into specific experiments to assess the goodness of UrbanSyn. Table III summarizes them. We run this table of experiments twice, i.e., to cover two significantly different deep models for semantic segmentation and their respective UDA procedures, namely, DeepLabV3+ (pure CNN-based model) and SegFormer MiT-B5 (Transformer-based model) with Co-training and HRDA

respective UDA procedures. Comparing experiments  $r - r - \text{Sup}$  with corresponding  $s - r - \text{Sup}$ , where  $r \in \{C, B, M\}$  and  $s \in \{G, S, U, GS, GSU\}$ , we can see domain gaps in accuracy for the supervised settings. Note that in the  $r - r - \text{Sup}$  experiments, real-world human-labeled images are used for training and there is no domain gap, thus, the resulting accuracy can be taken as an upper-bound reference. In the  $s - r - \text{Sup}$  experiments, synthetic-only automatically labeled images are used for training and there is a domain gap with the real-world images used for testing, thus, the resulting accuracy can be taken as a lower-bound reference or baseline. We can see how large the domain gap between given  $s$  and  $r$  is by comparing the accuracy resulting from the  $r - r - \text{Sup}$  and  $s - r - \text{Sup}$  experiments. In the UDA setting, we can see the contribution of the synthetic data  $s$  by comparing the accuracy of experiments  $s - r - \text{UDA}$  to  $s - r - \text{Sup}$  and  $r - r - \text{Sup}$ , varying  $r$  and the UDA method, where the aim is to approach (or surpass) the accuracy of  $r - r - \text{Sup}$  after significantly improving  $s - r - \text{Sup}$ . If we restrict  $s$  to a single synthetic dataset (here  $\{G, S, U\}$ ), we can compare their individual contributions. If  $s$  comes from the combination of different synthetic datasets, we can evaluate if they are complementary to the UDA task.

According to this standard setting of experiments, we will see in section IV-D that UrbanSyn allows to significantly increase the accuracy of different state-of-the-art synth-to-real UDA procedures for semantic segmentation (DeepLabV3+/Co-training, SegFormer MiT-B5/HRDA), in single-source regime—individually comparing UrbanSyn (U) to GTAV (G) and Synscapes (S)—and in a multi-source regime—comparing the use of GTAV+Synscapes+UrbanSyn (GSU) to only using GTAV+Synscapes (GS)—, and working with different real-world target domains—Cityscapes (C), BDD10K (B), Mapillary Vistas (M)—.

### B. Datasets and evaluation

The source (synthetic) datasets in common use to address synth-to-real UDA for semantic segmentation are GTAV [1], Synscapes [2], and SYNTHIA [4]. GTAV and Synscapes have semantic labeling for the 19 classes of Cityscapes [25], while this is not the case for SYNTHIA. Thus, since we are especially interested in a multi-source setting, in this paper, we define the Three Musketeers dataset as consisting of GTAV, Synscapes, and UrbanSyn. GTAV is composed of 24,966 images with a resolution of  $1914 \times 1052$  pixels directly obtained from the render engine of the videogame GTA V. Synscapes is composed of 25,000 images with a resolution of  $1440 \times 720$  pixels of urban scenes, obtained by using a physics-based rendering pipeline. UrbanSyn is composed of 7,539 images with a resolution of  $2048 \times 1024$  pixels.

As target (real-world) datasets, we not only consider Cityscapes [25] as in most previous literature but also the more challenging BDD100K [26] and Mapillary Vistas [27] datasets. Cityscapes is well-known for its semantic segmentation challenge, comprising 2,975 images for training and 500 for validation. The images have a resolution of  $2048 \times 1024$  pixels and were obtained from different cities in Germany. BDD100K

TABLE III: Types of experiments to be carried out. Each experiment ID gives rise to experiments based on different deep architectures for semantic segmentation, i.e., DeepLabV3+ and SegFormer in the supervised settings (Sup), including the respective Co-training and HRDA procedures in the UDA settings. For simplicity, we do not explicitly indicate these models and procedures in this table. We also indicate in which table of the paper the reader can find the respective experiments. Please, refer to the main text in section IV-A for details.

Experiment Type ID	$\mathcal{X}_s^\ell$	$\mathcal{X}_{R_r}^\ell$ from ...	$\mathcal{X}_{R_r}^u$ from ...	$\mathcal{X}_{R_t}^\ell$ from ...	Where?
Real-to-real supervised training (same domain)					
C-C-Sup	-	Cityscapes	-	Cityscapes	Table IV
B-B-Sup	-	BDD100K	-	BDD100K	Table V
M-M-Sup	-	Mapillary	-	Mapillary	Table VI
Synth-to-real supervised training (domain gap, no UDA)					
G-C-Sup	GTAV	-	-	Cityscapes	Table IV
G-B-Sup	GTAV	-	-	BDD100K	Table V
G-M-Sup	GTAV	-	-	Mapillary	Table VI
S-C-Sup	Synscapes	-	-	Cityscapes	Table IV
S-B-Sup	Synscapes	-	-	BDD100K	Table V
S-M-Sup	Synscapes	-	-	Mapillary	Table VI
U-C-Sup	UrbanSyn	-	-	Cityscapes	Table IV
U-B-Sup	UrbanSyn	-	-	BDD100K	Table V
U-M-Sup	UrbanSyn	-	-	Mapillary	Table VI
GS-C-Sup	GTAV + Synscapes	-	-	Cityscapes	Table IV
GS-B-Sup	GTAV + Synscapes	-	-	BDD100K	Table V
GS-M-Sup	GTAV + Synscapes	-	-	Mapillary	Table VI
GSU-C-Sup	GTAV + Synscapes + Urbansyn	-	-	Cityscapes	Table IV
GSU-B-Sup	GTAV + Synscapes + Urbansyn	-	-	BDD100K	Table V
GSU-M-Sup	GTAV + Synscapes + Urbansyn	-	-	Mapillary	Table VI
Synth-to-real UDA training (domain gap, self-labeling based UDA)					
G-C-UDA	GTAV	-	-	Cityscapes	Table IV
G-B-UDA	GTAV	-	-	BDD100K	Table V
G-M-UDA	GTAV	-	-	Mapillary	Table VI
S-C-UDA	Synscapes	-	-	Cityscapes	Table IV
S-B-UDA	Synscapes	-	-	BDD100K	Table V
S-M-UDA	Synscapes	-	-	Mapillary	Table VI
U-C-UDA	UrbanSyn	-	-	Cityscapes	Table IV
U-B-UDA	UrbanSyn	-	-	BDD100K	Table V
U-M-UDA	UrbanSyn	-	-	Mapillary	Table VI
GSU-C-UDA	GTAV + Synscapes + Urbansyn	-	-	Cityscapes	Table IV
GSU-B-UDA	GTAV + Synscapes + Urbansyn	-	-	BDD100K	Table V
GSU-M-UDA	GTAV + Synscapes + Urbansyn	-	-	Mapillary	Table VI

contains images taken from different vehicles in different USA cities. It is divided into 7,000 images for training and 1,000 for validation, with a resolution of  $1280 \times 720$  pixels. As in [16], for training purposes, we only use daytime images without heavy occlusions and favorable weather, resulting in a subset of 1,777 images. We consider the validation set as it comes. Mapillary Vistas is composed of a large number of images from around the world. These images were obtained with different camera devices, generating a large variety of resolutions and aspect ratios. Some images were captured onboard, and others were taken from personal devices at the street level. As in [16], we only consider images with an aspect ratio of 4:3, which comprises more than 75% of all the dataset images. This results in 14,716 images for training and 1,617 for validation.

For each model that we train, we assess its accuracy in the validation set of each real-world dataset according to the 19 official classes defined for Cityscapes. As is common practice, other classes are ignored. Model training in the synth-to-real UDA setting is performed by considering the synthetic datasets and the training set of each real-world dataset. The semantic labels of these real-world training images are ignored. These labels are just considered to train reference models, i.e., those trained and validated on the same real-world dataset domain.

TABLE IV: Target: Cityscapes. Per-class IoU and global mIoU values are shown. For each row, we report the mean and standard deviation based on three train-test runs. For each column, we highlight the best mean IoU/mIoU per **sub-block** (bold) and **block** (bold-underlined). Two means are highlighted as best if their difference is  $< 1$ .

Method	Source		Road	Sidewalk	Building	Wall	Fence	Pole	Traffic Light	Traffic Sign	Vegetation	Terrain	Sky	Person	Rider	Car	Truck	Bus	Train	Motorbike	Bike	mIoU
SegFormer	GTAV	mean	76.9	27.7	85.0	29.5	34.5	38.2	54.5	21.5	86.8	36.8	84.2	69.9	30.2	79.4	35.5	39.3	18.5	28.3	30.7	47.8
		std	$\pm 1.4$	$\pm 3.3$	$\pm 0.2$	$\pm 1.9$	$\pm 3.0$	$\pm 1.0$	$\pm 0.7$	$\pm 3.1$	$\pm 0.6$	$\pm 1.5$	$\pm 0.4$	$\pm 0.6$	$\pm 1.1$	$\pm 7.9$	$\pm 2.4$	$\pm 2.3$	$\pm 9.4$	$\pm 5.2$	$\pm 2.7$	$\pm 1.2$
SegFormer	Synscapes	mean	<b>91.9</b>	<b>49.4</b>	<b>78.9</b>	<b>36.4</b>	29.4	50.3	58.1	61.9	<b>86.9</b>	<b>38.1</b>	84.5	72.2	39.7	89.8	25.1	18.7	16.4	38.9	64.8	54.3
		std	$\pm 0.9$	$\pm 2.5$	$\pm 3.0$	$\pm 2.9$	$\pm 3.8$	$\pm 1.0$	$\pm 1.3$	$\pm 1.0$	$\pm 0.7$	$\pm 2.8$	$\pm 3.2$	$\pm 0.8$	$\pm 1.1$	$\pm 0.8$	$\pm 2.0$	$\pm 5.5$	$\pm 0.5$	$\pm 2.8$	$\pm 1.7$	$\pm 1.2$
SegFormer	UrbanSyn	mean	89.8	46.1	<b>87.3</b>	21.6	<b>47.6</b>	<b>56.4</b>	<b>64.0</b>	<b>69.6</b>	<b>87.2</b>	32.6	<b>88.5</b>	<b>77.2</b>	<b>54.9</b>	<b>93.1</b>	<b>69.1</b>	<b>65.3</b>	<b>28.5</b>	<b>50.0</b>	<b>73.2</b>	<b>63.3</b>
		std	$\pm 0.3$	$\pm 1.1$	$\pm 0.2$	$\pm 5.6$	$\pm 0.7$	$\pm 0.4$	$\pm 0.4$	$\pm 0.4$	$\pm 3.4$	$\pm 1.0$	$\pm 0.8$	$\pm 0.9$	$\pm 0.4$	$\pm 4.9$	$\pm 3.0$	$\pm 13.2$	$\pm 1.5$	$\pm 0.3$	$\pm 0.7$	$\pm 0.7$
SegFormer	GTAV+Synscapes	mean	90.5	50.9	<b>89.7</b>	47.9	47.4	54.0	65.5	54.8	<b>89.8</b>	47.4	<b>92.9</b>	74.0	37.4	90.6	46.2	64.3	<b>61.3</b>	52.6	62.9	64.2
		std	$\pm 1.2$	$\pm 3.0$	$\pm 0.1$	$\pm 2.3$	$\pm 0.7$	$\pm 0.4$	$\pm 0.2$	$\pm 1.9$	$\pm 0.4$	$\pm 2.9$	$\pm 0.2$	$\pm 0.4$	$\pm 3.4$	$\pm 0.5$	$\pm 2.9$	$\pm 1.6$	$\pm 5.8$	$\pm 3.2$	$\pm 2.3$	$\pm 0.8$
SegFormer	GTAV+Synscapes+UrbanSyn	mean	<b>92.3</b>	<b>57.7</b>	<b>90.3</b>	<b>50.2</b>	<b>53.2</b>	<b>58.1</b>	<b>66.7</b>	<b>67.8</b>	<b>90.0</b>	<b>48.5</b>	<b>91.0</b>	<b>79.8</b>	<b>56.5</b>	<b>93.2</b>	<b>71.3</b>	<b>77.1</b>	<b>60.3</b>	<b>61.4</b>	<b>73.5</b>	<b>70.5</b>
		std	$\pm 0.1$	$\pm 0.8$	$\pm 0.3$	$\pm 0.5$	$\pm 0.9$	$\pm 0.6$	$\pm 0.2$	$\pm 1.2$	$\pm 0.1$	$\pm 0.4$	$\pm 1.2$	$\pm 0.5$	$\pm 1.7$	$\pm 0.6$	$\pm 1.4$	$\pm 2.0$	$\pm 4.7$	$\pm 2.9$	$\pm 0.4$	$\pm 0.4$
HRDA (DAFormers)	GTAV	mean	90.3	32.1	<b>91.1</b>	<b>60.0</b>	52.8	58.2	64.7	71.9	<b>91.5</b>	48.2	<b>94.1</b>	75.0	22.9	94.0	83.2	73.4	19.3	65.2	66.5	66.0
		std	$\pm 3.8$	$\pm 27.4$	$\pm 0.1$	$\pm 1.3$	$\pm 2.2$	$\pm 1.2$	$\pm 0.2$	$\pm 0.5$	$\pm 1.3$	$\pm 0.1$	$\pm 2.7$	$\pm 21.0$	$\pm 0.1$	$\pm 0.9$	$\pm 8.2$	$\pm 27.3$	$\pm 0.5$	$\pm 0.7$	$\pm 4.9$	$\pm 4.9$
HRDA (DAFormers)	Synscapes	mean	<b>93.6</b>	<b>70.6</b>	89.1	45.9	49.5	<b>62.6</b>	<b>68.5</b>	64.6	90.5	<b>51.7</b>	<b>95.0</b>	77.8	39.4	93.5	63.8	47.3	65.3	53.9	<b>76.2</b>	68.4
		std	$\pm 1.1$	$\pm 3.7$	$\pm 1.3$	$\pm 1.7$	$\pm 9.9$	$\pm 0.4$	$\pm 1.1$	$\pm 3.5$	$\pm 0.3$	$\pm 3.3$	$\pm 0.0$	$\pm 0.5$	$\pm 2.5$	$\pm 0.6$	$\pm 7.2$	$\pm 10.4$	$\pm 0.2$	$\pm 0.9$	$\pm 0.9$	$\pm 0.9$
HRDA (DAFormers)	UrbanSyn	mean	90.5	56.1	<b>91.5</b>	<b>60.4</b>	<b>56.9</b>	<b>61.7</b>	66.2	<b>73.5</b>	<b>90.9</b>	46.4	<b>94.8</b>	<b>81.3</b>	<b>61.2</b>	<b>95.0</b>	<b>84.7</b>	<b>76.5</b>	38.1	63.9	<b>75.8</b>	<b>71.9</b>
		std	$\pm 0.1$	$\pm 0.3$	$\pm 0.3$	$\pm 1.1$	$\pm 0.6$	$\pm 0.9$	$\pm 0.2$	$\pm 0.2$	$\pm 2.2$	$\pm 0.1$	$\pm 0.4$	$\pm 0.1$	$\pm 0.0$	$\pm 3.0$	$\pm 4.8$	$\pm 3.1$	$\pm 1.4$	$\pm 0.4$	$\pm 0.7$	$\pm 0.7$
HRDA (DAFormers)	GTAV+Synscapes+UrbanSyn	mean	<b>97.0</b>	<b>77.8</b>	<b>92.0</b>	59.0	<b>57.0</b>	<b>63.1</b>	<b>68.4</b>	<b>75.3</b>	<b>91.9</b>	<b>55.5</b>	<b>94.9</b>	<b>81.4</b>	58.4	<b>94.9</b>	83.4	<b>88.4</b>	<b>75.4</b>	<b>65.7</b>	<b>76.1</b>	<b>76.6</b>
		std	$\pm 0.3$	$\pm 1.6$	$\pm 0.1$	$\pm 0.7$	$\pm 0.3$	$\pm 0.3$	$\pm 0.2$	$\pm 0.3$	$\pm 0.0$	$\pm 1.1$	$\pm 0.1$	$\pm 0.0$	$\pm 0.3$	$\pm 0.3$	$\pm 1.8$	$\pm 3.1$	$\pm 1.5$	$\pm 0.2$	$\pm 0.5$	$\pm 0.5$
SegFormer	Cityscapes (reference)	mean	98.5	87.1	93.5	65.8	65.4	68.5	74.7	81.9	93.1	64.9	95.5	84.2	66.3	95.7	84.0	91.5	84.1	72.8	79.7	81.5
		std	$\pm 0.0$	$\pm 0.1$	$\pm 0.2$	$\pm 2.6$	$\pm 1.1$	$\pm 0.2$	$\pm 0.3$	$\pm 0.3$	$\pm 0.1$	$\pm 1.3$	$\pm 0.1$	$\pm 0.1$	$\pm 0.6$	$\pm 0.2$	$\pm 2.5$	$\pm 0.8$	$\pm 1.9$	$\pm 1.0$	$\pm 0.1$	$\pm 0.1$
DeepLabV3+	GTAV	mean	68.7	26.3	71.9	<b>29.6</b>	23.9	33.6	41.4	17.2	83.9	31.2	50.3	64.7	25.3	64.8	30.2	18.0	0.3	20.3	20.2	38.0
		std	$\pm 7.7$	$\pm 2.7$	$\pm 2.5$	$\pm 2.7$	$\pm 0.5$	$\pm 1.1$	$\pm 0.6$	$\pm 1.4$	$\pm 0.3$	$\pm 2.3$	$\pm 4.9$	$\pm 0.9$	$\pm 3.0$	$\pm 15.7$	$\pm 2.4$	$\pm 3.9$	$\pm 0.1$	$\pm 1.6$	$\pm 5.3$	$\pm 0.6$
DeepLabV3+	Synscapes	mean	85.0	<b>42.4</b>	65.6	23.7	16.7	47.9	52.1	56.8	84.4	28.9	77.2	65.7	28.8	<b>86.3</b>	21.2	10.7	4.0	37.0	61.0	47.1
		std	$\pm 2.1$	$\pm 1.5$	$\pm 3.5$	$\pm 2.5$	$\pm 3.5$	$\pm 0.7$	$\pm 1.1$	$\pm 1.6$	$\pm 2.0$	$\pm 2.4$	$\pm 0.7$	$\pm 1.3$	$\pm 1.6$	$\pm 2.5$	$\pm 1.4$	$\pm 0.5$	$\pm 2.3$	$\pm 0.4$	$\pm 1.2$	$\pm 1.1$
DeepLabV3+	UrbanSyn	mean	<b>86.4</b>	<b>42.7</b>	<b>84.4</b>	25.4	<b>40.4</b>	<b>49.6</b>	<b>54.4</b>	<b>62.4</b>	<b>86.4</b>	<b>32.3</b>	<b>84.7</b>	<b>72.5</b>	<b>51.0</b>	76.1	<b>46.6</b>	<b>54.6</b>	<b>23.2</b>	<b>47.2</b>	<b>69.8</b>	<b>57.4</b>
		std	$\pm 0.6$	$\pm 1.1$	$\pm 0.6$	$\pm 3.8$	$\pm 1.5$	$\pm 0.6$	$\pm 0.0$	$\pm 0.1$	$\pm 1.4$	$\pm 0.7$	$\pm 0.5$	$\pm 1.1$	$\pm 3.8$	$\pm 3.7$	$\pm 10.9$	$\pm 5.8$	$\pm 1.3$	$\pm 0.3$	$\pm 1.3$	
DeepLabV3+	GTAV+Synscapes	mean	88.8	48.5	85.5	42.7	45.1	51.8	59.4	50.7	<b>88.7</b>	35.8	76.6	71.1	30.1	90.3	49.1	67.2	43.6	50.3	57.1	59.6
		std	$\pm 1.4$	$\pm 0.8$	$\pm 0.9$	$\pm 2.9$	$\pm 1.5$	$\pm 0.9$	$\pm 1.2$	$\pm 1.5$	$\pm 0.3$	$\pm 3.3$	$\pm 2.2$	$\pm 0.8$	$\pm 2.1$	$\pm 1.0$	$\pm 2.5$	$\pm 3.5$	$\pm 3.7$	$\pm 2.7$	$\pm 1.8$	$\pm 0.6$
DeepLabV3+	GTAV+Synscapes+UrbanSyn	mean	<b>90.7</b>	<b>52.3</b>	<b>88.9</b>	<b>48.5</b>	<b>50.6</b>	<b>57.6</b>	<b>63.6</b>	<b>64.7</b>	<b>89.6</b>	<b>44.6</b>	<b>91.6</b>	<b>77.5</b>	<b>54.2</b>	<b>91.8</b>	<b>64.7</b>	<b>75.5</b>	<b>56.5</b>	<b>55.6</b>	<b>71.2</b>	<b>67.9</b>
		std	$\pm 0.0$	$\pm 0.5$	$\pm 0.3$	$\pm 1.6$	$\pm 0.8$	$\pm 0.1$	$\pm 0.3$	$\pm 1.3$	$\pm 0.1$	$\pm 0.8$	$\pm 0.2$	$\pm 0.4$	$\pm 0.8$	$\pm 0.4$	$\pm 4.2$	$\pm 3.6$	$\pm 4.8$	$\pm 0.5$	$\pm 0.7$	$\pm 0.7$
Co-training (DeepLabV3+)	GTAV	mean	89.9	50.8	<b>89.2</b>	39.6	36.1	52.3	57.0	51.6	89.5	48.2	90.0	72.0	46.9	91.5	57.2	57.9	0.0	53.6	64.7	59.9
		std	$\pm 0.1$	$\pm 0.4$	$\pm 0.0$	$\pm 0.9$	$\pm 0.6$	$\pm 0.1$	$\pm 0.3$	$\pm 0.5$	$\pm 0.1$	$\pm 0.6$	$\pm 0.4$	$\pm 0.6$	$\pm 0.4$	$\pm 0.6$	$\pm 1.9$	$\pm 3.0$	$\pm 0.0$	$\pm 0.8$	$\pm 0.1$	$\pm 0.3$
Co-training (DeepLabV3+)	Synscapes	mean	<b>91.3</b>	<b>54.6</b>	82.4	36.7	43.6	<b>57.3</b>	<b>64.8</b>	69.5	<b>91.3</b>	<b>51.1</b>	<b>94.1</b>	77.3	41.4	<b>93.5</b>	17.2	19.6	1.7	<b>60.8</b>	<b>74.8</b>	59.1
		std	$\pm 0.1$	$\pm 0.5$	$\pm 0.1$	$\pm 0.3$	$\pm 0.2$	$\pm 0.3$	$\pm 0.2$	$\pm 0.3$	$\pm 0.1$	$\pm 0.4$	$\pm 0.1$	$\pm 0.2$	$\pm 1.6$	$\pm 0.1$	$\pm 1.1$	$\pm 0.2$	$\pm 0.1$	$\pm 0.9$	$\pm 0.3$	$\pm 0.1$
Co-training (DeepLabV3+)	UrbanSyn	mean	<b>91.8</b>	<b>53.9</b>	<b>88.9</b>	<b>40.9</b>	<b>51.2</b>	<b>56.7</b>	59.4	<b>71.3</b>	90.1	<b>51.5</b>	85.2	<b>80.7</b>	<b>60.0</b>	<b>94.3</b>	<b>79.4</b>	<b>83.7</b>	<b>62.4</b>	<b>61.7</b>	72.8	<b>70.3</b>
		std	$\pm 0.1$	$\pm 0.4$	$\pm 0.1$	$\pm 1.1$	$\pm 0.2$	$\pm 0.3$	$\pm 0.3$	$\pm 0.2$	$\pm 0.0$	$\pm 0.4$	$\pm 0.2$	$\pm 0.1$	$\pm 0.5$	$\pm 0.0$	$\pm 1.2$	$\pm 1.1$	$\pm 2.1$	$\pm 0.2$	$\pm 0.1$	$\pm 0.3$
Co-training (DeepLabV3+)	GTAV+Synscapes+UrbanSyn	mean	<b>96.8</b>	<b>76.9</b>	<b>91.8</b>	<b>56.4</b>	<b>58.3</b>	<b>62.4</b>	<b>67.4</b>	<b>75.0</b>	<b>91.7</b>	<b>57.2</b>	<b>94.6</b>	<b>82.1</b>	<b>62.0</b>	<b>94.8</b>	<b>82.7</b>	<b>90.0</b>	<b>76.4</b>	<b>65.2</b>	<b>75.0</b>	<b>76.7</b>
		std	$\pm 0.1$	$\pm 0.8$	$\pm 0.1$	$\pm 0.0$	$\pm 0.5$	$\pm 0.2$	$\pm 0.4$	$\pm 0.2$	$\pm 0.0$	$\pm 0.3$	$\pm 0.1$	$\pm 0.2$	$\pm 1.1$	$\pm 0.0$	$\pm 1.2$	$\pm 0.5$	$\pm 0.6$	$\pm 0.7$	$\pm 0.2$	$\pm 0.1$
DeepLabV3+	Cityscapes (reference)	mean	98.2	85.8	93.1	58.6	64.1	66.6	71.4	80.1	92.8	66.1	95.2	83.0	63.8	95.5	79.1	89.1	83.8	70.5	78.4	79.8
		std	$\pm 0.1$	$\pm 0.2$	$\pm 0.1$	$\pm 0.7$	$\pm 0.9$	$\pm 0.1$	$\pm 0.0$	$\pm 0.3$	$\pm 0.1$	$\pm 1.0$	$\pm 0.0$	$\pm 0.2$	$\pm 0.5$	$\pm 0.1$	$\pm 1.1$	$\pm 0.8$	$\pm 1.2$	$\pm 0.8$	$\pm 0.1$	$\pm 0.1$

As is standard, to assess segmentation accuracy, we use the intersection-over-union metric [73], i.e.,  $IoU = TP / (TP + FP + FN)$ , where TP, FP, and FN refer to true positives, false positives, and false negatives, respectively. Given a pixel

TABLE V: Analogous to Table IV but for BDD100K as target. (\*) The bad results on the class Train are due to inconsistencies in the validation set labeling as we will illustrate in Section IV-E.

Method	Source		Road	Sidewalk	Building	Wall	Fence	Pole	Traffic Light	Traffic Sign	Vegetation	Terrain	Sky	Person	Rider	Car	Truck	Bus	Train*	Motorbike	Bike	mIoU
SegFormer	GTAV	mean	76.2	25.9	75.8	8.8	35.0	39.2	42.0	24.8	72.2	35.1	88.3	55.6	26.2	74.8	26.7	13.2	0.0	41.0	21.9	41.2
		std	$\pm 2.9$	$\pm 0.6$	$\pm 0.4$	$\pm 3.1$	$\pm 1.7$	$\pm 0.2$	$\pm 1.2$	$\pm 1.5$	$\pm 1.3$	$\pm 0.7$	$\pm 0.6$	$\pm 0.6$	$\pm 1.6$	$\pm 5.5$	$\pm 1.3$	$\pm 2.6$	$\pm 0.0$	$\pm 1.8$	$\pm 6.7$	$\pm 0.2$
SegFormer	Synscapes	mean	79.8	29.9	62.6	2.9	15.8	29.9	27.9	32.9	73.6	20.2	86.1	49.4	18.2	72.8	10.3	13.7	0.0	38.9	41.3	37.2
		std	$\pm 2.6$	$\pm 0.6$	$\pm 1.2$	$\pm 0.1$	$\pm 2.7$	$\pm 1.1$	$\pm 0.8$	$\pm 1.1$	$\pm 0.8$	$\pm 2.3$	$\pm 0.8$	$\pm 1.3$	$\pm 1.9$	$\pm 2.3$	$\pm 1.5$	$\pm 3.3$	$\pm 0.0$	$\pm 3.3$	$\pm 3.6$	$\pm 0.3$
SegFormer	UrbanSyn	mean	86.3	24.1	63.2	4.6	25.4	40.6	39.8	40.1	65.6	19.7	78.6	45.7	22.6	82.7	21.7	51.3	0.0	38.6	34.3	41.3
		std	$\pm 0.8$	$\pm 3.9$	$\pm 2.3$	$\pm 0.4$	$\pm 5.9$	$\pm 0.3$	$\pm 1.2$	$\pm 1.5$	$\pm 2.2$	$\pm 2.4$	$\pm 1.7$	$\pm 2.6$	$\pm 3.8$	$\pm 0.1$	$\pm 2.2$	$\pm 4.2$	$\pm 0.1$	$\pm 1.6$	$\pm 4.2$	$\pm 0.8$
SegFormer	GTAV+Synscapes	mean	82.4	31.6	78.7	18.4	38.0	43.0	45.1	30.1	76.8	35.8	89.4	61.4	24.2	76.2	30.5	44.9	0.0	52.4	50.1	47.8
		std	$\pm 3.8$	$\pm 1.2$	$\pm 1.0$	$\pm 1.0$	$\pm 0.8$	$\pm 0.9$	$\pm 1.0$	$\pm 1.6$	$\pm 0.6$	$\pm 0.5$	$\pm 0.6$	$\pm 0.6$	$\pm 2.1$	$\pm 4.0$	$\pm 1.4$	$\pm 11.7$	$\pm 0.0$	$\pm 1.5$	$\pm 3.1$	$\pm 1.2$
SegFormer	GTAV+Synscapes+UrbanSyn	mean	87.7	37.8	80.1	18.1	37.0	45.5	46.8	42.1	75.1	36.5	89.2	62.0	41.6	82.3	35.0	45.8	0.0	56.8	59.2	51.5
		std	$\pm 1.4$	$\pm 2.6$	$\pm 0.1$	$\pm 4.1$	$\pm 1.8$	$\pm 0.2$	$\pm 0.6$	$\pm 1.0$	$\pm 1.0$	$\pm 1.6$	$\pm 0.7$	$\pm 1.5$	$\pm 5.3$	$\pm 2.1$	$\pm 1.6$	$\pm 2.9$	$\pm 0.0$	$\pm 0.6$	$\pm 1.2$	$\pm 0.5$
HRDA (DAFormer)	GTAV	mean	90.0	28.2	81.3	29.9	38.6	42.6	48.2	38.6	80.6	41.3	91.3	60.5	38.5	85.2	42.1	65.0	0.0	43.1	34.1	51.5
		std	$\pm 0.9$	$\pm 10.8$	$\pm 0.5$	$\pm 2.0$	$\pm 1.0$	$\pm 0.4$	$\pm 0.1$	$\pm 0.4$	$\pm 2.2$	$\pm 0.2$	$\pm 0.6$	$\pm 3.8$	$\pm 0.5$	$\pm 2.1$	$\pm 3.2$	$\pm 0.0$	$\pm 4.1$	$\pm 2.7$	$\pm 1.2$	$\pm 1.2$
HRDA (DAFormer)	Synscapes	mean	61.5	18.8	78.1	9.0	15.9	38.6	43.4	26.3	79.4	16.3	91.3	58.2	27.5	85.1	25.7	49.1	0.0	46.4	51.4	43.3
		std	$\pm 24.6$	$\pm 9.2$	$\pm 1.0$	$\pm 4.6$	$\pm 5.6$	$\pm 1.0$	$\pm 1.4$	$\pm 1.7$	$\pm 0.7$	$\pm 10.6$	$\pm 0.5$	$\pm 2.1$	$\pm 0.9$	$\pm 1.6$	$\pm 9.6$	$\pm 6.4$	$\pm 0.0$	$\pm 2.4$	$\pm 0.6$	$\pm 2.9$
HRDA (DAFormer)	UrbanSyn	mean	92.1	45.9	81.0	8.3	40.2	43.7	49.1	53.6	81.7	42.9	91.4	64.5	34.4	87.9	45.0	69.2	0.0	44.0	54.1	54.2
		std	$\pm 0.4$	$\pm 1.1$	$\pm 0.4$	$\pm 3.1$	$\pm 1.3$	$\pm 0.8$	$\pm 0.6$	$\pm 0.5$	$\pm 0.4$	$\pm 2.2$	$\pm 0.3$	$\pm 2.4$	$\pm 7.9$	$\pm 3.3$	$\pm 1.4$	$\pm 1.4$	$\pm 0.0$	$\pm 10.2$	$\pm 6.5$	$\pm 0.8$
HRDA (DAFormer)	GTAV+Synscapes+UrbanSyn	mean	90.5	56.7	82.6	29.3	41.8	49.5	52.5	52.4	82.7	43.8	92.7	67.0	47.5	81.9	49.8	76.1	0.0	55.1	62.0	58.6
		std	$\pm 0.5$	$\pm 0.9$	$\pm 0.1$	$\pm 1.1$	$\pm 1.8$	$\pm 0.1$	$\pm 1.1$	$\pm 0.9$	$\pm 0.3$	$\pm 0.6$	$\pm 0.2$	$\pm 1.3$	$\pm 2.5$	$\pm 1.5$	$\pm 1.0$	$\pm 3.1$	$\pm 0.0$	$\pm 1.7$	$\pm 1.0$	$\pm 0.4$
SegFormer	BDD100K (reference)	mean	95.0	66.1	87.2	34.2	52.7	51.0	56.8	57.4	87.4	53.0	95.8	66.4	29.7	90.7	61.3	81.8	0.0	48.7	52.8	61.5
		std	$\pm 0.1$	$\pm 0.6$	$\pm 0.0$	$\pm 0.2$	$\pm 0.1$	$\pm 0.4$	$\pm 0.5$	$\pm 0.3$	$\pm 0.1$	$\pm 1.0$	$\pm 0.2$	$\pm 0.6$	$\pm 12.7$	$\pm 0.5$	$\pm 1.1$	$\pm 2.0$	$\pm 0.0$	$\pm 7.9$	$\pm 3.8$	$\pm 1.2$
DeepLabV3+	GTAV	mean	63.6	25.9	59.4	6.3	27.6	32.3	36.0	21.3	66.2	21.1	77.1	52.2	16.9	68.2	18.4	17.9	0.0	29.0	6.1	34.0
		std	$\pm 3.7$	$\pm 1.8$	$\pm 2.5$	$\pm 0.5$	$\pm 2.1$	$\pm 0.8$	$\pm 0.5$	$\pm 1.7$	$\pm 0.6$	$\pm 3.0$	$\pm 2.6$	$\pm 1.3$	$\pm 1.9$	$\pm 1.2$	$\pm 1.0$	$\pm 1.5$	$\pm 0.0$	$\pm 7.3$	$\pm 1.8$	$\pm 0.1$
DeepLabV3+	Synscapes	mean	66.5	21.1	32.9	1.1	5.1	22.3	25.3	23.2	61.9	6.5	57.3	47.3	17.9	63.3	1.6	5.7	0.0	30.8	34.0	27.6
		std	$\pm 5.4$	$\pm 2.5$	$\pm 3.7$	$\pm 0.5$	$\pm 0.8$	$\pm 2.8$	$\pm 0.9$	$\pm 1.5$	$\pm 3.8$	$\pm 0.4$	$\pm 6.5$	$\pm 3.5$	$\pm 3.4$	$\pm 2.3$	$\pm 0.6$	$\pm 0.5$	$\pm 0.0$	$\pm 2.5$	$\pm 4.2$	$\pm 1.1$
DeepLabV3+	UrbanSyn	mean	80.1	29.3	64.8	3.3	15.8	33.6	31.3	33.2	74.1	24.2	79.5	42.5	22.4	68.7	19.6	22.6	0.0	45.3	50.6	39.0
		std	$\pm 1.6$	$\pm 1.4$	$\pm 0.8$	$\pm 0.2$	$\pm 0.1$	$\pm 0.3$	$\pm 0.4$	$\pm 0.6$	$\pm 0.3$	$\pm 1.6$	$\pm 1.0$	$\pm 7.8$	$\pm 8.0$	$\pm 1.4$	$\pm 1.7$	$\pm 5.2$	$\pm 0.0$	$\pm 0.6$	$\pm 1.2$	$\pm 0.5$
DeepLabV3+	GTAV+Synscapes	mean	67.2	30.2	74.7	12.9	29.9	37.7	39.9	27.7	75.0	25.1	86.5	57.9	37.1	62.0	20.7	25.0	0.1	47.5	50.5	42.5
		std	$\pm 1.3$	$\pm 2.3$	$\pm 0.9$	$\pm 3.0$	$\pm 2.1$	$\pm 2.0$	$\pm 2.5$	$\pm 0.9$	$\pm 0.3$	$\pm 1.6$	$\pm 1.0$	$\pm 1.6$	$\pm 3.4$	$\pm 1.6$	$\pm 0.1$	$\pm 1.6$	$\pm 0.0$	$\pm 1.8$	$\pm 5.2$	$\pm 1.1$
DeepLabV3+	GTAV+Synscapes+UrbanSyn	mean	78.8	34.7	76.4	11.2	32.6	36.9	37.0	29.5	75.8	33.1	87.7	56.9	26.5	71.2	25.6	45.1	0.0	47.1	55.8	45.4
		std	$\pm 0.2$	$\pm 1.5$	$\pm 0.5$	$\pm 1.5$	$\pm 2.1$	$\pm 0.4$	$\pm 0.3$	$\pm 0.4$	$\pm 0.7$	$\pm 0.1$	$\pm 0.5$	$\pm 0.6$	$\pm 2.9$	$\pm 1.5$	$\pm 0.3$	$\pm 2.3$	$\pm 0.0$	$\pm 0.1$	$\pm 1.4$	$\pm 0.5$
Co-training (DeepLabV3+)	GTAV	mean	82.7	56.0	77.9	20.8	41.7	36.9	34.9	19.7	74.8	37.4	87.5	54.8	40.3	71.3	27.5	4.5	0.4	38.4	19.1	43.5
		std	$\pm 0.1$	$\pm 1.1$	$\pm 0.3$	$\pm 0.2$	$\pm 1.4$	$\pm 0.1$	$\pm 0.8$	$\pm 0.4$	$\pm 0.0$	$\pm 0.2$	$\pm 0.9$	$\pm 0.5$	$\pm 0.3$	$\pm 0.6$	$\pm 0.2$	$\pm 0.4$	$\pm 0.5$	$\pm 3.6$	$\pm 0.3$	$\pm 0.3$
Co-training (DeepLabV3+)	Synscapes	mean	89.9	35.5	52.7	1.5	6.9	39.5	32.2	25.9	78.6	25.5	77.2	60.5	30.2	85.5	1.7	29.6	0.0	50.3	54.4	40.9
		std	$\pm 0.1$	$\pm 0.2$	$\pm 0.4$	$\pm 0.1$	$\pm 0.3$	$\pm 0.1$	$\pm 0.2$	$\pm 0.2$	$\pm 0.2$	$\pm 1.1$	$\pm 0.6$	$\pm 0.5$	$\pm 4.5$	$\pm 0.1$	$\pm 0.3$	$\pm 0.0$	$\pm 0.0$	$\pm 2.4$	$\pm 0.5$	$\pm 0.3$
Co-training (DeepLabV3+)	UrbanSyn	mean	90.5	36.3	76.9	10.0	29.2	31.2	30.1	32.3	74.8	37.7	88.7	47.8	44.8	86.7	37.7	65.4	0.0	37.1	43.1	47.4
		std	$\pm 0.0$	$\pm 0.9$	$\pm 0.3$	$\pm 0.0$	$\pm 0.8$	$\pm 0.3$	$\pm 0.8$	$\pm 0.7$	$\pm 0.2$	$\pm 0.3$	$\pm 0.1$	$\pm 4.3$	$\pm 1.9$	$\pm 0.1$	$\pm 1.5$	$\pm 2.6$	$\pm 0.0$	$\pm 0.7$	$\pm 1.7$	$\pm 0.3$
Co-training (DeepLabV3+)	GTAV+Synscapes+UrbanSyn	mean	92.1	44.4	81.1	24.2	44.1	43.2	46.6	40.3	72.4	36.4	87.0	64.0	57.7	87.5	46.0	76.9	0.7	51.1	55.7	55.3
		std	$\pm 0.1$	$\pm 0.6$	$\pm 0.1$	$\pm 2.2$	$\pm 0.6$	$\pm 0.1$	$\pm 0.2$	$\pm 0.1$	$\pm 0.2$	$\pm 0.6$	$\pm 0.1$	$\pm 0.7$	$\pm 1.4$	$\pm 0.0$	$\pm 0.7$	$\pm 0.7$	$\pm 0.2$	$\pm 0.5$	$\pm 0.9$	$\pm 0.1$
DeepLabV3+	BDD100K (reference)	mean	94.7	65.7	86.5	36.1	53.8	50.9	54.4	55.4	86.8	50.7	95.1	65.0	45.9	90.6	59.7	81.0	0.0	47.6	43.4	61.2
		std	$\pm 0.1$	$\pm 0.1$	$\pm 0.1$	$\pm 0.9$	$\pm 0.6$	$\pm 0.3$	$\pm 2.2$	$\pm 0.2$	$\pm 0.2$	$\pm 0.5$	$\pm 0.1$	$\pm 0.6$	$\pm 2.9$	$\pm 0.1$	$\pm 0.8$	$\pm 1.9$	$\pm 0.0$	$\pm 3.0$	$\pm 3.5$	$\pm 0.3$

## D. Results analysis

This analysis relies on the results reported in Tables IV, V, and VI, which correspond to Cityscapes, BDD100K, and Mapillary Vistas, respectively. Each table has a block for approaches based on DeepLabV3+ and another for those based on SegFormer, each including sub-blocks (separated by horizontal lines) for baselines, UDA, and the block reference (training and testing in the same real-world domain).

Comparing the individual performance of UrbanSyn, GTAV, and Synscapes, we see that the best per-class accuracy is not always given by the same dataset. However, in terms of mIoU, UrbanSyn is the best performing in all cases (always for DeepLabV3+; with Cityscapes and Mapillary Vistas for SegFormer) but one (with BDD100K for SegFormer, in pair with GTAV). The same outcome is observed when applying single-source synth-to-real UDA. In terms of baselines, we see that by adding UrbanSyn to GTAV and Synscapes, the mIoU increases significantly: 6.3 points for SegFormer/Cityscapes, 8.3 for DeepLabV3+/Cityscapes, 3.7 for SegFormer/BDD100K, 2.9 for DeepLabV3+/BDD100K, 6.0 for SegFormer/Mapillary Vistas, 7.7 for DeepLabV3+/Mapillary Vistas. Finally, we see that Musketeers is also beneficial for synth-to-real UDA. For Cityscapes, HRDA reaches mIoU=76.6, which is just 4.9 points behind its reference, while co-training reaches mIoU=76.7, just 3.1 points behind its reference. For BDD100K, HRDA reaches mIoU=58.6, 2.9 points behind its reference, while co-training reaches mIoU=55.3, 5.9 points

behind its reference. For Mapillary Vistas, HRDA reaches mIoU=68.0, 11.5 points behind its reference, while co-training reaches mIoU=68.8, 8.4 points behind its reference.

It is noticeable that Musketeers with HRDA (without ImageNet distance loss) reach mIoU=76.6 for Cityscapes, which is the new synth-to-real state-of-the-art to the best of our knowledge. The mIoU=75.2 reached by co-training is 5.0 points better than the results reported in [16]. For the case of BDD100K and Mapillary Vistas, co-training improves 5.2 and 7.5 points from the results reported in [16].

Figure 7 illustrates how UrbanSyn is helping to provide stronger baselines as part of the Musketeers, no matter if we use DeepLabV3+ or SegFormer. For Cityscapes, UrbanSyn helps to better separate the road from the sidewalk; for B

TABLE VI: Analogous to Table IV but for Mapillary Vistas as target.

Method	Source		Road	Sidewalk	Building	Wall	Fence	Pole	Traffic Light	Traffic Sign	Vegetation	Terrain	Sky	Person	Rider	Car	Truck	Bus	Train	Motorbike	Bike	mIoU
SegFormer	GTAV	mean	83.3	40.2	83.9	32.0	41.4	43.4	53.1	53.4	77.6	43.1	<b>94.8</b>	70.1	31.9	86.2	49.3	42.0	<b>21.1</b>	43.6	22.3	53.3
		std	$\pm 1.9$	$\pm 3.1$	$\pm 0.1$	$\pm 1.4$	$\pm 0.8$	$\pm 0.5$	$\pm 1.1$	$\pm 1.7$	$\pm 1.3$	$\pm 3.2$	$\pm 0.1$	$\pm 0.8$	$\pm 1.6$	$\pm 1.4$	$\pm 2.0$	$\pm 5.1$	$\pm 4.5$	$\pm 2.4$	$\pm 0.4$	$\pm 0.8$
SegFormer	Synscapes	mean	83.6	39.0	72.1	27.0	26.2	39.1	50.2	66.8	<b>81.4</b>	<b>49.5</b>	93.3	64.6	43.8	83.5	30.2	8.6	1.9	49.3	59.2	51.0
		std	$\pm 2.3$	$\pm 3.7$	$\pm 1.0$	$\pm 2.6$	$\pm 3.0$	$\pm 1.8$	$\pm 1.6$	$\pm 0.7$	$\pm 0.8$	$\pm 1.3$	$\pm 0.7$	$\pm 2.0$	$\pm 3.6$	$\pm 2.8$	$\pm 2.2$	$\pm 3.4$	$\pm 1.1$	$\pm 1.7$	$\pm 0.7$	$\pm 0.8$
SegFormer	UrbanSyn	mean	<b>88.0</b>	33.2	73.6	13.5	<b>44.5</b>	<b>49.6</b>	<b>59.2</b>	<b>69.2</b>	80.2	48.2	91.2	<b>74.3</b>	<b>55.8</b>	<b>89.3</b>	<b>52.1</b>	<b>52.5</b>	<b>21.0</b>	<b>58.0</b>	<b>64.0</b>	<b>58.8</b>
		std	$\pm 0.8$	$\pm 4.6$	$\pm 3.0$	$\pm 2.7$	$\pm 1.4$	$\pm 0.2$	$\pm 0.4$	$\pm 0.4$	$\pm 0.8$	$\pm 0.8$	$\pm 1.8$	$\pm 0.2$	$\pm 4.2$	$\pm 0.3$	$\pm 2.9$	$\pm 6.9$	$\pm 2.5$	$\pm 1.3$	$\pm 1.5$	$\pm 0.3$
SegFormer	GTAV+Synscapes	mean	86.6	46.8	85.7	38.3	46.0	47.5	58.5	60.3	<b>79.8</b>	<b>48.2</b>	<b>95.5</b>	75.4	51.5	89.2	56.3	56.4	28.8	55.5	55.8	61.2
		std	$\pm 0.4$	$\pm 1.7$	$\pm 0.1$	$\pm 2.3$	$\pm 1.6$	$\pm 0.6$	$\pm 0.5$	$\pm 1.3$	$\pm 0.8$	$\pm 1.0$	$\pm 0.1$	$\pm 0.4$	$\pm 3.1$	$\pm 0.2$	$\pm 2.4$	$\pm 3.2$	$\pm 8.6$	$\pm 1.8$	$\pm 4.5$	$\pm 0.5$
SegFormer	GTAV+Synscapes+UrbanSyn	mean	<b>90.1</b>	<b>53.3</b>	<b>86.7</b>	<b>42.2</b>	<b>52.4</b>	<b>51.8</b>	<b>62.3</b>	<b>68.8</b>	<b>80.4</b>	<b>48.3</b>	<b>95.6</b>	<b>77.5</b>	<b>61.1</b>	<b>91.8</b>	<b>68.3</b>	<b>69.6</b>	<b>52.3</b>	<b>59.8</b>	<b>63.6</b>	<b>67.2</b>
		std	$\pm 0.8$	$\pm 2.3$	$\pm 0.2$	$\pm 1.0$	$\pm 1.6$	$\pm 0.5$	$\pm 0.3$	$\pm 0.3$	$\pm 0.2$	$\pm 0.8$	$\pm 0.1$	$\pm 0.8$	$\pm 0.2$	$\pm 0.2$	$\pm 2.2$	$\pm 3.7$	$\pm 5.1$	$\pm 1.1$	$\pm 0.6$	$\pm 0.6$
HRDA (DAFormer*)	GTAV	mean	<b>85.5</b>	<b>21.0</b>	<b>86.6</b>	<b>46.0</b>	35.2	47.3	58.0	62.4	66.0	36.5	92.3	65.0	21.7	89.1	58.7	64.2	5.6	14.8	0.0	50.3
		std	$\pm 0.8$	$\pm 7.0$	$\pm 1.1$	$\pm 0.9$	$\pm 0.9$	$\pm 0.4$	$\pm 1.6$	$\pm 8.1$	$\pm 13.6$	$\pm 1.1$	$\pm 9.7$	$\pm 18.6$	$\pm 0.8$	$\pm 1.1$	$\pm 5.7$	$\pm 58.0$	$\pm 9.8$	$\pm 55.5$	$\pm 62.3$	$\pm 56.8$
HRDA (DAFormer*)	Synscapes	mean	<b>84.6</b>	12.8	74.6	26.1	<b>43.4</b>	46.8	51.0	65.5	<b>87.8</b>	<b>42.2</b>	<b>92.8</b>	68.6	51.3	89.2	56.7	58.0	9.8	55.5	62.3	<b>56.8</b>
		std	$\pm 3.1$	$\pm 12.3$	$\pm 10.1$	$\pm 1.4$	$\pm 3.5$	$\pm 2.7$	$\pm 5.9$	$\pm 1.9$	$\pm 0.7$	$\pm 27.6$	$\pm 6.7$	$\pm 6.2$	$\pm 5.2$	$\pm 1.1$	$\pm 6.6$	$\pm 5.7$	$\pm 5.1$	$\pm 4.1$	$\pm 4.6$	$\pm 5.1$
HRDA (DAFormer*)	UrbanSyn	mean	80.1	7.2	85.2	7.9	35.0	<b>50.0</b>	<b>63.4</b>	<b>74.1</b>	74.2	0.0	<b>93.4</b>	<b>78.4</b>	<b>57.0</b>	<b>90.8</b>	<b>66.4</b>	<b>69.8</b>	<b>29.0</b>	<b>57.8</b>	<b>67.7</b>	<b>57.2</b>
		std	$\pm 3.4$	$\pm 9.8$	$\pm 0.3$	$\pm 9.4$	$\pm 10.0$	$\pm 0.1$	$\pm 0.3$	$\pm 0.7$	$\pm 1.7$	$\pm 1.0$	$\pm 0.3$	$\pm 0.2$	$\pm 1.0$	$\pm 0.5$	$\pm 1.4$	$\pm 4.9$	$\pm 16.5$	$\pm 2.0$	$\pm 6.8$	$\pm 1.9$
HRDA (DAFormer*)	GTAV+Synscapes+UrbanSyn	mean	<b>88.3</b>	<b>55.4</b>	<b>88.4</b>	<b>49.1</b>	49.7	<b>52.2</b>	<b>63.9</b>	<b>75.9</b>	<b>86.9</b>	<b>61.1</b>	<b>97.2</b>	<b>78.7</b>	<b>60.9</b>	<b>91.7</b>	<b>71.3</b>	<b>52.7</b>	<b>44.4</b>	<b>58.9</b>	<b>65.4</b>	<b>68.0</b>
		std	$\pm 4.7$	$\pm 5.1$	$\pm 0.2$	$\pm 1.2$	$\pm 1.2$	$\pm 0.5$	$\pm 0.3$	$\pm 0.2$	$\pm 0.6$	$\pm 0.2$	$\pm 0.3$	$\pm 0.3$	$\pm 2.0$	$\pm 0.1$	$\pm 1.0$	$\pm 31.1$	$\pm 6.0$	$\pm 1.6$	$\pm 0.6$	$\pm 2.2$
SegFormer	Mapillary Vistas (reference)	mean	96.8	82.1	92.2	60.9	71.0	67.1	73.0	83.3	92.5	75.6	98.7	81.0	64.9	93.9	80.0	87.6	68.2	67.8	73.5	79.5
		std	$\pm 0.1$	$\pm 0.1$	$\pm 0.3$	$\pm 4.7$	$\pm 1.4$	$\pm 0.8$	$\pm 0.5$	$\pm 0.1$	$\pm 0.0$	$\pm 0.3$	$\pm 0.0$	$\pm 0.1$	$\pm 0.1$	$\pm 0.1$	$\pm 0.1$	$\pm 0.6$	$\pm 4.5$	$\pm 0.4$	$\pm 0.2$	$\pm 0.7$
DeeplabV3+	GTAV	mean	68.4	29.5	55.6	18.9	32.2	34.9	<b>46.3</b>	46.4	75.8	34.3	75.2	<b>68.1</b>	30.8	<b>81.0</b>	38.7	12.7	11.4	32.1	23.6	43.0
		std	$\pm 2.8$	$\pm 1.9$	$\pm 3.7$	$\pm 2.8$	$\pm 0.4$	$\pm 1.9$	$\pm 0.9$	$\pm 1.5$	$\pm 0.6$	$\pm 0.8$	$\pm 3.4$	$\pm 1.0$	$\pm 0.6$	$\pm 1.6$	$\pm 0.5$	$\pm 1.3$	$\pm 3.5$	$\pm 1.0$	$\pm 2.0$	$\pm 1.1$
DeeplabV3+	Synscapes	mean	67.6	<b>30.7</b>	45.0	10.8	10.2	34.2	38.7	<b>56.1</b>	73.4	<b>39.1</b>	78.7	57.6	35.8	76.8	7.3	4.3	0.2	39.6	<b>52.4</b>	39.9
		std	$\pm 1.2$	$\pm 0.8$	$\pm 2.6$	$\pm 1.1$	$\pm 0.7$	$\pm 1.0$	$\pm 1.2$	$\pm 1.3$	$\pm 0.9$	$\pm 1.4$	$\pm 0.5$	$\pm 1.0$	$\pm 2.2$	$\pm 1.1$	$\pm 0.8$	$\pm 0.0$	$\pm 1.3$	$\pm 1.9$	$\pm 0.4$	$\pm 0.4$
DeeplabV3+	UrbanSyn	mean	<b>78.8</b>	26.1	<b>72.8</b>	10.4	<b>34.2</b>	<b>37.7</b>	<b>43.3</b>	<b>56.3</b>	<b>81.0</b>	36.1	<b>87.8</b>	<b>67.7</b>	<b>46.4</b>	66.1	<b>42.1</b>	<b>33.2</b>	<b>15.3</b>	<b>42.5</b>	<b>51.0</b>	<b>48.9</b>
		std	$\pm 0.6$	$\pm 1.5$	$\pm 1.2$	$\pm 0.9$	$\pm 0.6$	$\pm 0.9$	$\pm 0.7$	$\pm 0.4$	$\pm 0.6$	$\pm 0.9$	$\pm 1.1$	$\pm 0.4$	$\pm 0.6$	$\pm 0.4$	$\pm 0.5$	$\pm 0.7$	$\pm 3.2$	$\pm 0.9$	$\pm 0.3$	$\pm 0.4$
DeeplabV3+	GTAV+Synscapes	mean	72.9	33.3	80.2	24.7	36.5	42.9	57.5	58.0	<b>78.3</b>	41.0	92.6	73.5	39.8	<b>87.3</b>	46.9	49.3	12.1	52.3	48.6	53.8
		std	$\pm 2.2$	$\pm 2.1$	$\pm 1.1$	$\pm 4.5$	$\pm 0.7$	$\pm 1.1$	$\pm 0.5$	$\pm 4.3$	$\pm 0.4$	$\pm 2.4$	$\pm 1.2$	$\pm 1.1$	$\pm 0.5$	$\pm 0.9$	$\pm 1.7$	$\pm 2.3$	$\pm 4.7$	$\pm 2.4$	$\pm 1.2$	$\pm 1.4$
DeeplabV3+	GTAV+Synscapes+UrbanSyn	mean	<b>86.9</b>	<b>50.9</b>	<b>83.1</b>	<b>32.2</b>	<b>44.7</b>	<b>50.4</b>	<b>59.4</b>	<b>66.8</b>	<b>78.5</b>	<b>43.5</b>	<b>94.4</b>	<b>76.1</b>	<b>52.9</b>	<b>87.9</b>	<b>58.0</b>	<b>61.4</b>	<b>18.5</b>	<b>58.4</b>	<b>65.3</b>	<b>61.5</b>
		std	$\pm 0.7$	$\pm 0.8$	$\pm 0.3$	$\pm 0.5$	$\pm 1.0$	$\pm 0.3$	$\pm 0.6$	$\pm 0.7$	$\pm 0.4$	$\pm 0.5$	$\pm 0.3$	$\pm 0.2$	$\pm 1.1$	$\pm 0.5$	$\pm 1.4$	$\pm 1.8$	$\pm 3.0$	$\pm 1.1$	$\pm 0.4$	$\pm 0.5$
Co-training (DeepLabV3+)	GTAV	mean	<b>88.2</b>	<b>44.2</b>	<b>85.3</b>	<b>31.8</b>	35.5	<b>49.3</b>	<b>58.0</b>	63.1	75.8	51.2	93.2	<b>74.4</b>	50.6	<b>88.7</b>	51.5	31.3	<b>11.8</b>	46.4	45.9	56.6
		std	$\pm 0.1$	$\pm 0.1$	$\pm 0.1$	$\pm 0.8$	$\pm 0.3$	$\pm 0.3$	$\pm 0.3$	$\pm 0.3$	$\pm 0.3$	$\pm 0.2$	$\pm 0.5$	$\pm 0.1$	$\pm 0.2$	$\pm 0.6$	$\pm 0.3$	$\pm 1.6$	$\pm 2.5$	$\pm 0.6$	$\pm 0.6$	$\pm 0.3$
Co-training (DeepLabV3+)	Synscapes	mean	78.0	36.3	73.5	16.9	33.8	<b>48.4</b>	56.0	71.0	<b>86.5</b>	<b>56.6</b>	<b>96.6</b>	<b>74.4</b>	38.6	<b>88.6</b>	0.6	18.5	0.2	48.5	59.5	51.7
		std	$\pm 0.2$	$\pm 0.2$	$\pm 0.0$	$\pm 0.0$	$\pm 0.2$	$\pm 0.9$	$\pm 0.5$	$\pm 0.1$	$\pm 0.0$	$\pm 0.0$	$\pm 0.1$	$\pm 1.6$	$\pm 0.1$	$\pm 0.1$	$\pm 0.1$	$\pm 0.1$	$\pm 0.0$	$\pm 0.4$	$\pm 0.0$	$\pm 0.2$
Co-training (DeepLabV3+)	UrbanSyn	mean	80.0	36.6	84.1	24.5	<b>44.5</b>	<b>47.5</b>	<b>58.6</b>	<b>73.3</b>	83.4	43.1	<b>96.5</b>	<b>74.0</b>	<b>59.7</b>	63.4	<b>63.5</b>	<b>69.9</b>	7.8	<b>57.2</b>	<b>63.8</b>	<b>59.5</b>
		std	$\pm 0.1$	$\pm 0.2$	$\pm 0.1$	$\pm 0.4$	$\pm 0.1$	$\pm 0.1$	$\pm 0.2$	$\pm 0.2$	$\pm 0.1$	$\pm 0.1$	$\pm 0.0$	$\pm 0.5$	$\pm 0.9$	$\pm 0.4$	$\pm 1.9$	$\pm 1.5$	$\pm 1.3$	$\pm 1.3$	$\pm 0.2$	$\pm 0.1$
Co-training (DeepLabV3+)	GTAV+Synscapes+UrbanSyn	mean	<b>91.7</b>	<b>55.2</b>	<b>87.2</b>	<b>42.3</b>	<b>56.1</b>	<b>54.1</b>	<b>66.6</b>	<b>74.7</b>	<b>86.2</b>	<b>57.8</b>	<b>97.1</b>	<b>79.1</b>	<b>59.9</b>	<b>92.6</b>	<b>70.1</b>	<b>75.4</b>	<b>32.0</b>	<b>61.5</b>	<b>68.5</b>	<b>68.8</b>
		std	$\pm 0.1$	$\pm 0.6$	$\pm 0.0$	$\pm 0.6$	$\pm 0.1$	$\pm 0.2$	$\pm 0.4$	$\pm 0.1$	$\pm 0.0$	$\pm 0.2$	$\pm 0.0$	$\pm 0.1$	$\pm 0.4$	$\pm 0.0$	$\pm 0.6$	$\pm 0.8$	$\pm 2.7$	$\pm 1.3$	$\pm 0.9$	$\pm 0.2$
DeeplabV3+	Mapillary Vistas (reference)	mean	96.4	79.8	91.0	57.0	68.4	65.6	71.8	82.6	92.2	73.8	98.6	80.9	64.2	93.7	77.2	81.0	56.6	64.6	71.3	77.2
		std	$\pm 0.2$	$\pm 0.9$	$\pm 0.1$	$\pm 0.8$	$\pm 0.2$	$\pm 0.1$	$\pm 0.1$	$\pm 0.3$	$\pm 0.0$	$\pm 0.6$	$\pm 0.0$	$\pm 0.7$	$\pm 1.8$	$\pm 0.2$	$\pm 0.3$	$\pm 1.2$	$\pm 2.9$	$\pm 1.7$	$\pm 1.0$	$\pm 0.4$

## E. Erroneous human labels

During the qualitative analysis of the results, we observed labeling errors in the ground truth of the real-world datasets. For instance, the BDD100K validation set only contains seven images (out of 1,000 images) with labels of the Train class. In five of these, the samples are extremely challenging (Figure 8), while in the other two, the labels are just wrong (Figure 9). Analyzing the BDD100K training set, we found only 27 images with labels of the Train class (out of 7

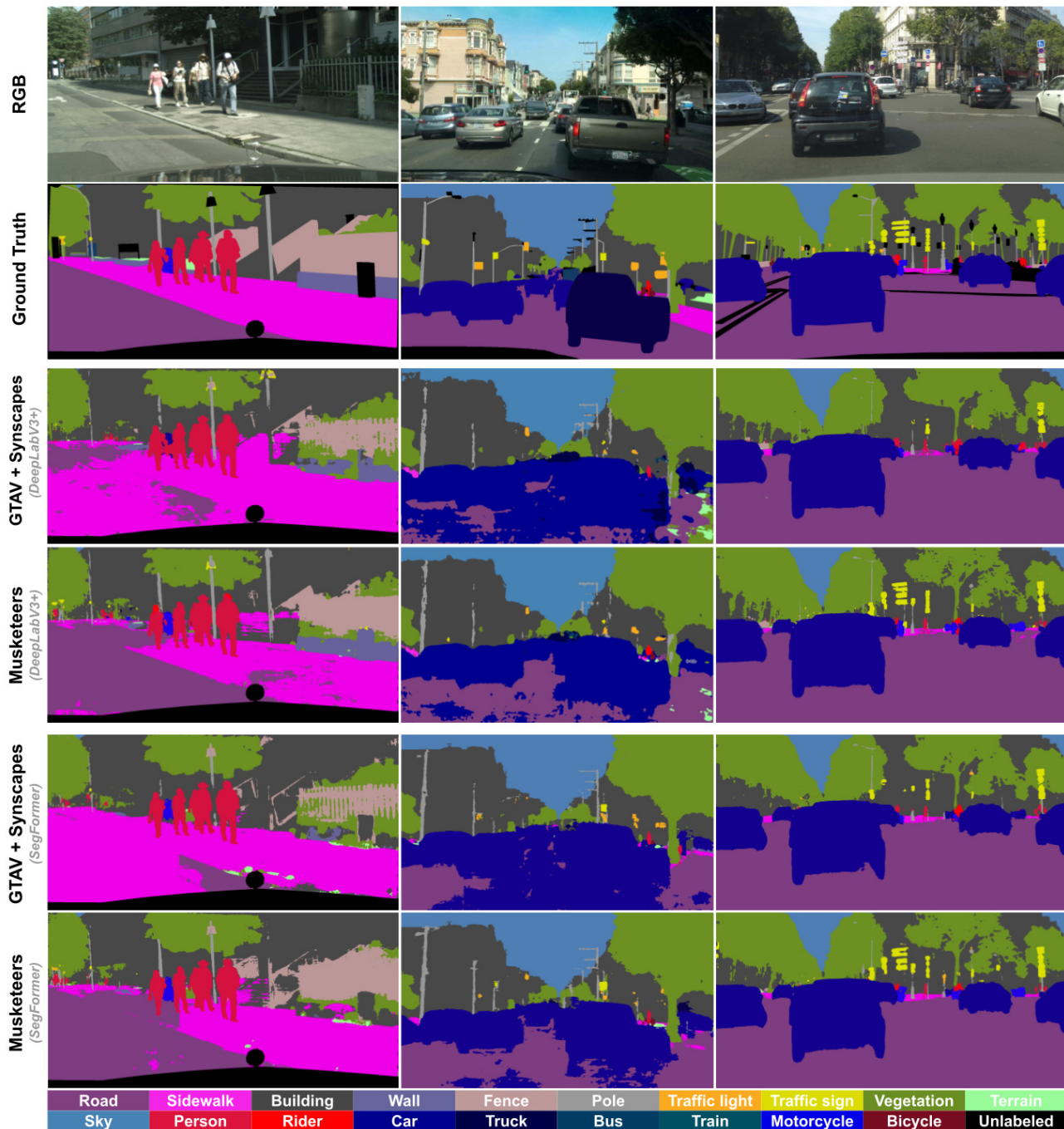


Fig. 7: From left to right, each column considers Cityscapes, BDD100K, and Mapillary Vistas. We show three blocks of two rows. First: RGB images and semantic ground truth. Second: semantic segmentation inference using DeepLabV3+, training with GTA+Synscapes and with the Musketeers (+UrbanSyn). Third: as the second block but using SegFormer.

the motorbike/bike form the same instance) and GTAV-based instances (no bikes/cyclists are included, and motorbike riders are treated as pedestrians). In addition, as future work, we want to explore how UrbanSyn can help in synth-to-real active learning procedures, where, in contrast to UDA, this approach allows for a certain budget to label a few real-world training images by hand. The challenge lies in selecting which images to allocate that budget.

#### ACCESSING THE DATASET

In order to download UrbanSyn, users have two options, either accessing the UrbanSyn web page, <https://urbansyn.org>, or accessing the popular HuggingFace services, <https://huggingface.co/datasets/UrbanSyn/UrbanSyn>. Both sites include all the information required to download the data, a description of their content, and visual examples.



Fig. 8: BDD100K images from the validation set containing very challenging Train class samples (encircled in red).



Fig. 9: BDD100K images from the validation set containing wrong labels of the Train class (encircled in red).



Fig. 10: Left to right: RGB image from Cityscapes' validation set, its semantic ground truth, and its co-training inference. Human labeling misses Traffic Light and Traffic Sign instances that co-training labels (boxed in red). In addition, a rider in the bottom right of the image is incorrectly labeled as a Pedestrian by humans, while co-training identifies it as Rider + Bicycle.

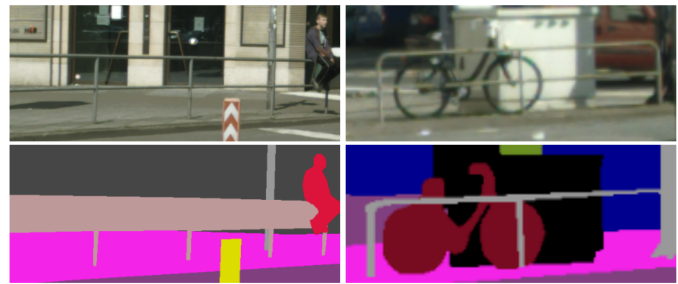


Fig. 11: Cityscapes images from the validation set containing inconsistencies in human labeling for the Fence class. Note how different criteria have been used to label the Fences in the left and right images.



Fig. 12: The closest Traffic Light instance is fully labeled as such (in yellow the lightbox and its support), while for the further away only the light boxes are labeled as Traffic Light.

#### ACKNOWLEDGEMENTS

This work has been supported by the Spanish grants Ref. PID2020-115734RB-C21 (ADA/SSL-ADA subproject) and PID2020-115734RB-C22 (ADA/PGAS-ADA subproject), both funded by MCIN/AEI/10.13039/501100011033. Antonio M. López acknowledges the financial support to his general research activities given by ICREA under the ICREA Academia Program. CVC's authors acknowledge the support of the Generalitat de Catalunya CERCA Program and its ACCIO agency to CVC's general activities. Jose A. Iglesias-Guitian acknowledges the financial support to his general research activities given by UDC-Inditex InTalent programme, the Spanish Ministry of Science and Innovation (AEI/RYC2018-025385-I), and Xunta de Galicia (ED431F 2021/11, EU-FEDER ED431G 2019/01).

## REFERENCES

- [1] S. R. Richter, V. Vineet, S. Roth, and V. Koltun, "Playing for data: Ground truth from computer games," in *European Conference on Computer Vision (ECCV)*, 2016.
- [2] M. Wrenninge and J. Unger, "Synscapes: A photorealistic synthetic dataset for street scene parsing," arXiv:1810.08705, 2018.
- [3] A. Gaidon, Q. Wang, Y. Cabon, and E. Vig, "Virtual worlds as proxy for multi-object tracking analysis," in *Int. Conf. on Computer Vision and Pattern Recognition (CVPR)*, 2016.
- [4] G. Ros, L. Sellart, J. Materzyska, D. Vázquez, and A. López, "The SYNTHIA dataset: a large collection of synthetic images for semantic segmentation of urban scenes," in *Int. Conf. on Computer Vision and Pattern Recognition (CVPR)*, 2016.
- [5] M. Wang and W. Deng, "Deep visual domain adaptation: A survey," *Neurocomputing*, vol. 312, no. 27, pp. 135–153, 2018.
- [6] G. Wilson and D. J. Cook, "A survey of unsupervised deep domain adaptation," *ACM Transactions on Intelligent Systems and Technology*, vol. 11, no. 5, pp. 1–46, 2020.
- [7] G. Csurka, T. M. Hospedales, M. Salzmann, and T. Tommasi, *Visual domain adaptation in the deep learning era*, ser. Synthesis Lectures on Computer Vision. Morgan & Claypool Publishers, 2022, vol. 11, no. 1.
- [8] W. Yang, K. Lu, P. Yang, and J. Lin, "Critically examining the "neural hype": Weak baselines and the additivity of effectiveness gains from neural ranking models," in *International ACM SIGIR Conference on Research and Development in Information Retrieval*, 2019.
- [9] M. Ferrari, P. Cremonesi, and D. Jannach, "Are we really making much progress? a worrying analysis of recent neural recommendation approaches," in *ACM Conference on Recommender Systems (RecSys)*, 2019.
- [10] J. Lambert, Z. Liu, O. Sener, J. Hays, and V. Koltun, "MSeg: A composite dataset for multi-domain semantic segmentation," in *Int. Conf. on Computer Vision and Pattern Recognition (CVPR)*, 2020.
- [11] X. Zhou, V. Koltun, and P. Krähenbühl, "Simple multi-dataset detection," in *Int. Conf. on Computer Vision and Pattern Recognition (CVPR)*, 2022.
- [12] R. Ranftl, K. Lasinger, D. Hafner, K. Schindler, and V. Koltun, "Towards robust monocular depth estimation: Mixing datasets for zero-shot cross-dataset transfer," *IEEE Trans. on Pattern Analysis and Machine Intelligence*, vol. 44, pp. 1623–1637, 2022.
- [13] R. Gong, D. Dai, Y. Chen, W. Li, and L. Van Gool, "mDALU: Multi-source domain adaptation and label unification with partial datasets," in *International Conference on Computer Vision (ICCV)*, 2021.
- [14] S. Zhao, B. Li, X. Yue, Y. Gu, P. Xu, R. Hu, H. Chai, and K. Keutzer, "Multi-source domain adaptation for semantic segmentation," in *Neural Information Processing Systems (NeurIPS)*, 2019.
- [15] J. He, X. Jia, S. Chen, and J. Liu, "Multi-source domain adaptation with collaborative learning for semantic segmentation," in *Int. Conf. on Computer Vision and Pattern Recognition (CVPR)*, 2021.
- [16] J. Gómez, G. Villalonga, and A. López, "Co-training for unsupervised domain adaptation of semantic segmentation models," *Sensors*, vol. 23, p. 621, 2023.
- [17] A. Garcia-Garcia, S. Orts-Escolano, S. Oprea, V. Villena-Martinez, P. Martinez-Gonzalez, and J. Garcia-Rodriguez, "A survey on deep learning techniques for image and video semantic segmentation," *Applied Soft Computing*, vol. 70, pp. 41–65, 2018.
- [18] G. Csurka, R. Volpi, and B. Chidlovskii, "Semantic image segmentation: Two decades of research," *Foundations and Trends in Computer Graphics and Vision*, vol. 14, pp. 1–162, 2022.
- [19] Y. Mo, Y. Wu, X. Yang, F. Liu, and Y. Liao, "Review the state-of-the-art technologies of semantic segmentation based on deep learning," *Neurocomputing*, vol. 493, pp. 626–646, 2022.
- [20] J. Janai, F. Guney, A. Behl, and A. Geiger, "Computer vision for autonomous vehicles: Problems, datasets and state-of-the-art," *Foundations and Trends in Computer Graphics and Vision*, vol. 12, pp. 1–308, 2020.
- [21] A. Tampuu, T. Matisen, M. Semikin, D. Fishman, and N. Muhammad, "A survey of end-to-end driving: Architectures and training methods," *IEEE Transactions on Neural Networks and Learning Systems*, vol. 33, pp. 1364–1384, 2020.
- [22] L.-H. Wen and K.-H. Jo, "Deep learning-based perception systems for autonomous driving: A comprehensive survey," *Neurocomputing*, vol. 489, pp. 255–270, 2022.
- [23] L.-C. Chen, G. Papandreou, I. Kokkinos, K. Murphy, and A. Yuille, "DeepLab: Semantic image segmentation with deep convolutional nets, atrous convolution, and fully connected crfs," *IEEE Trans. on Pattern Analysis and Machine Intelligence*, vol. 40, pp. 834–848, 2017.
- [24] E. Xie, W. Wang, Z. Yu, A. Anandkumar, J. Alvarez, and P. Luo, "SegFormer: Simple and efficient design for semantic segmentation with transformers," in *Neural Information Processing Systems (NeurIPS)*, 2021.
- [25] M. Cordts, M. Omran, S. Ramos, T. Rehfeld, M. Enzweiler, R. Benenson, U. Franke, S. Roth, and B. Schiele, "The Cityscapes dataset for semantic urban scene understanding," in *Int. Conf. on Computer Vision and Pattern Recognition (CVPR)*, 2016.
- [26] F. Yu, H. Chen, X. Wang, W. Xian, Y. Chen, F. Liu, V. Madhavan, and T. Darrell, "BDD100K: A diverse driving dataset for heterogeneous multitask learning," in *Int. Conf. on Computer Vision and Pattern Recognition (CVPR)*, 2020.
- [27] G. Neuhold, T. Ollmann, S. R. Bulò, and P. Kotschieder, "The Mapillary Vistas dataset for semantic understanding of street scenes," in *International Conference on Computer Vision (ICCV)*, 2017.
- [28] L. Hoyer, D. Dai, and L. Van Gool, "HRDA: Context-aware high-resolution domain-adaptive semantic segmentation," in *European Conference on Computer Vision (ECCV)*, 2022.
- [29] A. Tsirikoglou, G. Eilertsen, and J. Unger, "A survey of image synthesis methods for visual machine learning," *Computer Graphics Forum*, vol. 39, no. 6, pp. 426–451, 2020.
- [30] S. Shah, D. Dey, C. Lovett, and A. Kapoor, "Airsim: High-fidelity visual and physical simulation for autonomous vehicles," in *Field and Service Robotics: Results of the 11th International Conference*. Springer, 2018, pp. 621–635.
- [31] M. Roberts, J. Ramapuram, A. Ranjan, A. Kumar, M. A. Bautista, N. Paczan, R. Webb, and J. M. Susskind, "Hypersim: A photorealistic synthetic dataset for holistic indoor scene understanding," in *International Conference on Computer Vision (ICCV)*, 2021.
- [32] H. Fu, R. Jia, L. Gao, M. Gong, B. Zhao, S. Maybank, and D. Tao, "3D-future: 3D furniture shape with texture," *International Journal of Computer Vision*, vol. 129, pp. 3313–3337, 2021.
- [33] M. Savva, A. Kadian, O. Maksymets, Y. Zhao, E. Wijmans, B. Jain, J. Straub, J. Liu, V. Koltun, J. Malik *et al.*, "Habitat: A platform for embodied ai research," in *International Conference on Computer Vision (ICCV)*, 2019.
- [34] V. Haltakov, C. Unger, and S. Ilic, "Framework for generation of synthetic ground truth data for driver assistance applications," in *German Conference on Pattern Recognition (GCPR)*, 2013.
- [35] M. Johnson-Roberson, C. Barto, R. Mehta, S. N. Sridhar, K. Rosaen, and R. Vasudevan, "Driving in the matrix: Can virtual worlds replace human-generated annotations for real world tasks?" arXiv:1610.01983, 2016.
- [36] A. Dosovitskiy, G. Ros, F. Codevilla, A. López, and V. Koltun, "CARLA: an open urban driving simulator," in *Conference on Robot Learning (CoRL)*, 2017.
- [37] H. Blasinski, J. Farrell, T. Lian, Z. Liu, and B. Wandell, "Optimizing image acquisition systems for autonomous driving," *Electronic Imaging*, vol. 2018, no. 5, pp. 161–1, 2018.
- [38] S. Khan, B. Phan, R. Salay, and K. Czarnecki, "ProcSy: Procedural synthetic dataset generation towards influence factor studies of semantic segmentation networks," in *Int. Conf. on Computer Vision and Pattern Recognition (CVPR)–Workshops*, 2019.
- [39] Y. I. Parish and P. Müller, "Procedural modeling of cities," in *Conference on Computer graphics and interactive techniques*, 2001.
- [40] A. Kar, A. Prakash, M.-Y. Liu, E. Cameracci, J. Yuan, M. Rusiniak, D. Acuna, A. Torralba, and S. Fidler, "Meta-sim: Learning to generate synthetic datasets," in *International Conference on Computer Vision (ICCV)*, 2019.
- [41] J. Devaranjan, A. Kar, and S. Fidler, "Meta-Sim2: Learning to generate synthetic datasets," in *European Conference on Computer Vision (ECCV)*, 2020.
- [42] Y. Luo, L. Zheng, T. Guan, J. Yu, and Y. Yang, "Taking a closer look at domain shift: Category-level adversaries for semantics consistent domain adaptation," in *Int. Conf. on Computer Vision and Pattern Recognition (CVPR)*, 2019.
- [43] C. Qin, L. Wang, Y. Zhang, and Y. Fu, "Generatively inferential co-training for unsupervised domain adaptation," in *International Conference on Computer Vision (ICCV) Workshops*, 2019.
- [44] J. Choi, T. Kim, and C. Kim, "Self-ensembling with gan-based data augmentation for domain adaptation in semantic segmentation," in *International Conference on Computer Vision (ICCV)*, 2019.
- [45] Y.-H. Tsai, K. Sohn, S. Schuster, and M. Chandraker, "Domain adaptation for structured output via discriminative patch representations," in *International Conference on Computer Vision (ICCV)*, 2019.
- [46] T.-H. Vu, H. Jain, M. Bucher, M. Cord, and P. Perez, "Advent: Adversarial entropy minimization for domain adaptation in semantic

- segmentation,” in *Int. Conf. on Computer Vision and Pattern Recognition (CVPR)*, 2019.
- [47] F. Lv, T. Liang, X. Chen, and G. Lin, “Cross-domain semantic segmentation via domain-invariant interactive relation transfer,” in *Int. Conf. on Computer Vision and Pattern Recognition (CVPR)*, 2020.
- [48] M. Kim and H. Byun, “Learning texture invariant representation for domain adaptation of semantic segmentation,” in *Int. Conf. on Computer Vision and Pattern Recognition (CVPR)*, 2020.
- [49] Z. Wang, M. Yu, Y. Wei, R. Feris, J. Xiong, W.-m. Hwu, T. Huang, and H. Shi, “Differential treatment for stuff and things: A simple unsupervised domain adaptation method for semantic segmentation,” in *Int. Conf. on Computer Vision and Pattern Recognition (CVPR)*, 2020.
- [50] H. Wang, T. Shen, W. Zhang, L.-Y. Duan, and T. Mei, “Classes matter: A fine-grained adversarial approach to cross-domain semantic segmentation,” in *European Conference on Computer Vision (ECCV)*, 2020.
- [51] L. Gao, J. Zhang, L. Zhang, and D. Tao, “DSP: Dual soft-paste for unsupervised domain adaptive semantic segmentation,” in *ACM International Conference on Multimedia*, 2021.
- [52] Z. Zheng and Y. Yang, “Rectifying pseudo label learning via uncertainty estimation for domain adaptive semantic segmentation,” *International Journal of Computer Vision*, vol. 129, p. 1106–1120, 2021.
- [53] L. Hoyer, D. Dai, and L. Van Gool, “DAFormer: Improving network architectures and training strategies for domain-adaptive semantic segmentation,” in *Int. Conf. on Computer Vision and Pattern Recognition (CVPR)*, 2022.
- [54] H.-S. Hong, A. Kumar, and D.-G. Lee, “Robust unsupervised domain adaptation by retaining confident entropy via edge concatenation,” *Expert Systems with Applications*, vol. 238, p. 122120, 2024.
- [55] Y. Li, L. Yuan, and N. Vasconcelos, “Bidirectional learning for domain adaptation of semantic segmentation,” in *Int. Conf. on Computer Vision and Pattern Recognition (CVPR)*, 2019.
- [56] Y. Zou, Z. Yu, X. Liu, B. Kumar, and J. Wang, “Confidence regularized self-training,” in *International Conference on Computer Vision (ICCV)*, 2019.
- [57] M. Subhani and M. Ali, “Learning from scale-invariant examples for domain adaptation in semantic segmentation,” in *European Conference on Computer Vision (ECCV)*, 2020.
- [58] C.-H. Chao, B.-W. Cheng, and C.-Y. Lee, “Rethinking ensemble-distillation for semantic segmentation based unsupervised domain adaptation,” in *Int. Conf. on Computer Vision and Pattern Recognition (CVPR)*, 2021.
- [59] K. Zhang, Y. Sun, R. Wang, H. Li, and X. Hu, “Multiple fusion adaptation: A strong framework for unsupervised semantic segmentation adaptation,” in *British Machine Vision Conference (BMVC)*, 2021.
- [60] W. Tranheden, V. Olsson, J. Pinto, and L. Svensson, “DACs: Domain adaptation via cross-domain mixed sampling,” in *Winter conf. on Applications of Computer Vision (WACV)*, 2021.
- [61] V. Olsson, W. Tranheden, J. Pinto, and L. Svensson, “ClassMix: Segmentation-based data augmentation for semi-supervised learning,” in *Winter conf. on Applications of Computer Vision (WACV)*, 2021.
- [62] N. Araslanov and S. Roth, “Self-supervised augmentation consistency for adapting semantic segmentation,” in *Int. Conf. on Computer Vision and Pattern Recognition (CVPR)*, 2021.
- [63] Y. Zou, Z. Yu, B. Kumar, and J. Wang, “Unsupervised domain adaptation for semantic segmentation via class-balanced self-training,” in *European Conference on Computer Vision (ECCV)*, 2018.
- [64] W.-L. Chang, W.-H. Wang, Hui-Po Peng, and W.-C. Chiu, “All about structure: Adapting structural information across domains for boosting semantic segmentation,” in *Int. Conf. on Computer Vision and Pattern Recognition (CVPR)*, 2019.
- [65] Y. Yang and S. Soatto, “FDA: Fourier domain adaptation for semantic segmentation,” in *Int. Conf. on Computer Vision and Pattern Recognition (CVPR)*, 2020.
- [66] K. De and M. Pedersen, “Impact of colour on robustness of deep neural networks,” in *Int. Conf. on Computer Vision and Pattern Recognition (CVPR)*, 2020.
- [67] R. D. Caballar, “The way we write software has unappreciated environmental impacts,” *IEEE Spectrum*, pp. 26–31, April 2024.
- [68] J. T. Kajiya, “The rendering equation,” in *Proceedings of the 13th annual conference on Computer graphics and interactive techniques*, 1986, pp. 143–150.
- [69] A. Keller, L. Fascione, M. Fajardo, I. Georgiev, P. Christensen, J. Hanika, C. Eisenacher, and G. Nichols, “The path tracing revolution in the movie industry,” in *ACM SIGGRAPH 2015 Courses*. ACM, 2015, pp. 1–7.
- [70] M. Zwicker, W. Jarosz, J. Lehtinen, B. Moon, R. Ramamoorthi, F. Rouselle, P. Sen, C. Soler, and S.-E. Yoon, “Recent advances in adaptive sampling and reconstruction for monte carlo rendering,” in *Computer graphics forum*, vol. 34, no. 2, 2015, pp. 667–681.
- [71] Y. Huo and S.-e. Yoon, “A survey on deep learning-based monte carlo denoising,” *Computational visual media*, vol. 7, pp. 169–185, 2021.
- [72] A. Prakash, S. Boochoon, M. Brophy, D. Acuna, E. Cameracci, G. State, O. Shapira, and S. Birchfield, “Structured domain randomization: Bridging the reality gap by context-aware synthetic data,” in *2019 International Conference on Robotics and Automation (ICRA)*. IEEE, 2019, pp. 7249–7255.
- [73] M. Everingham, S. Eslami, L. Van Gool, C. K. Williams, J. Winn, and A. Zisserman, “The PASCAL visual object classes challenge: A retrospective,” *International Journal of Computer Vision*, vol. 111, no. 1, pp. 98–136, 2015.
- [74] Y. Wu, A. Kirillov, F. Massa, W.-Y. Lo, and R. Girshick, “Detectron2,” <https://github.com/facebookresearch/detectron2>, 2019.
- [75] M. Contributors, “MMSegmentation: Openmmlab semantic segmentation toolbox and benchmark,” <https://github.com/open-mmlab/mms Segmentation>, 2020.